Received: 16 December 2021 | Revised: 8 September 2022 | Accepted: 13 September 2022

DOI: 10.1002/esp.5481

RESEARCH ARTICLE

ESPL WILEY

# Aeolization on the Atlantic coast of Galicia (NW Spain) from the end of the last glacial period to the present day: Chronology, origin and evolution of coastal dunes linked to sea-level oscillations

Carlos Arce Chamorro | Juan Ramón Vidal Romaní | Aurora Grandal d'Anglade | Jorge Sanjurjo Sánchez

Grupo interdisciplinar de Patrimonio Cultural y Geológico 'CULXEO', Instituto Universitario de Geología 'Isidro Parga Pondal', Universidad de A Coruña, ESCI, A Coruña, Spain

**Correspondence**
Carlos Arce Chamorro, Grupo interdisciplinar de Patrimonio Cultural y Geológico 'CULXEO', Instituto Universitario de Geología 'Isidro Parga Pondal', Universidad de A Coruña, ESCI, Campus de Elviña, 15071 A Coruña, Spain.
Email: carlos.arce@udc.es

**Funding information**
Consellería de Cultura, Educación e Ordenación Universitaria, Xunta de Galicia (ED431B 2018/47 and ED431B 2021/17). Funding for Open Acces: Universidade da Coruña/CISUG

## Abstract

The Atlantic coast of Galicia (NW Spain) is a high-energy environment where shingle beaches are currently developing. These coarser sediments alternate with sandy deposits which are also considered as beaches typical of a low-energy environment. The physical association of both types of sediment with contrasted sedimentary significance raises problems of interpretation. The study of four outcrops of fossil aeolianites on this coast has allowed us to reconstruct their evolution from the end of the Upper Pleistocene to the present day. Their chronology, estimated by optically stimulated luminescence between 35 and 14 ky at the end of the last glaciation (MIS2), coincides with a local sea level 120 m below the present one. This implies a coastline shifted several kilometres from its current location and the subaerial exposure of a wide strip of the continental shelf covered by sands. The wind blew sand to form dunes towards the continent, covering the coastal areas, which then emerged with no other limitation than the active river channels. Sea-level rise during the Holocene transgression has progressively swamped these aeolian deposits, leaving only flooded dunes, relict coastal dunes and climbing dunes on cliffs up to 180 m high. The aeolian process continued as long as there was a sandy source area to erode, although accretion finished when the sea reached its current level (Late Holocene). Since then, the wind turned from accretion to erosion of the dunes and sand beaches. This erosion exposes the older shingle beaches (probably of Eemian age) buried under the aeolian sands, as well as old, submerged forest remains and megalithic monuments. The destruction of sand beaches and dunes currently observed along the Galician coast is linked, according to most researchers, to anthropogenic global warming. However, their management should consider these evolutive issues.

KEYWORDS
aeolian accretion, coastal aeolianites, glacio-eustasy, NW Spanish Atlantic coast, optically stimulated luminescence, Upper Pleistocene and Holocene

## 1 | INTRODUCTION

The management of coastal dunes with regard to the most extreme climatic events of today depends largely on the degree of knowledge of their evolution (Muñoz-Vallés & Cambrollé, 2014), especially in areas such as NW Spain (Figure 1), where coastal dunes are relict and vulnerable formations (Gutiérrez-Becker, 2008) that are strongly affected by wave action (Flor-Blanco et al., 2021), as observed in other areas of the southern half of the European Atlantic coast (Brown et al., 2014; De Winter & Ruessink, 2017; Loureiro et al., 2012; Vousdoukas et al., 2012). This would enhance its environmental and scientific value (Costa-Casais & Caetano-Alves, 2013; Marrero-Rodríguez & Dóniz-Páez, 2022; Reynard et al., 2007), as coastal dunes represent key sediments for the reconstruction of coastal evolution linked to sea-level oscillations since the end of the last glacial period (Vidal-Romaní & Grandal-d'Anglade, 2018). Coastal dunes were already recognized as points of geological interest (Duque et al., 1983), but unfortunately many of them have been severely affected by sand extraction and urban constructions in recent times.

The evolution of the Galician Atlantic coast (NW Spain) (Figure 1) during the last glacial event (Upper Pleistocene) and the Holocene transgression is poorly understood due to the lack of an accurate interpretation. Generally, the local record is characterized by the absence of suitable absolute ages or the lack of detailed sedimentological and/or micropaleontological studies (Mosquera-Santé, 2000) that would allow a more precise description of the evolution of this coast. The abundant literature during the last three decades (Durán, 2005; García-Gil et al., 1999, 2020; García-Moreiras et al., 2019; Méndez & Vilas, 2005; Muñoz-Sobrino et al., 2016; Rey-Salgado, 1993) has not provided significant progress. Stratigraphic sequences from the marine drillings (by vibrocorer or gravity) on the surface of the continental shelf and the seabed of the Galician Rias (Figure 1) have not achieved an understanding of the coastal evolution during glacio-eustatic variations. This is due to the interpretation of isolated data (Costas et al., 2009; González-Villanueva et al., 2015) or

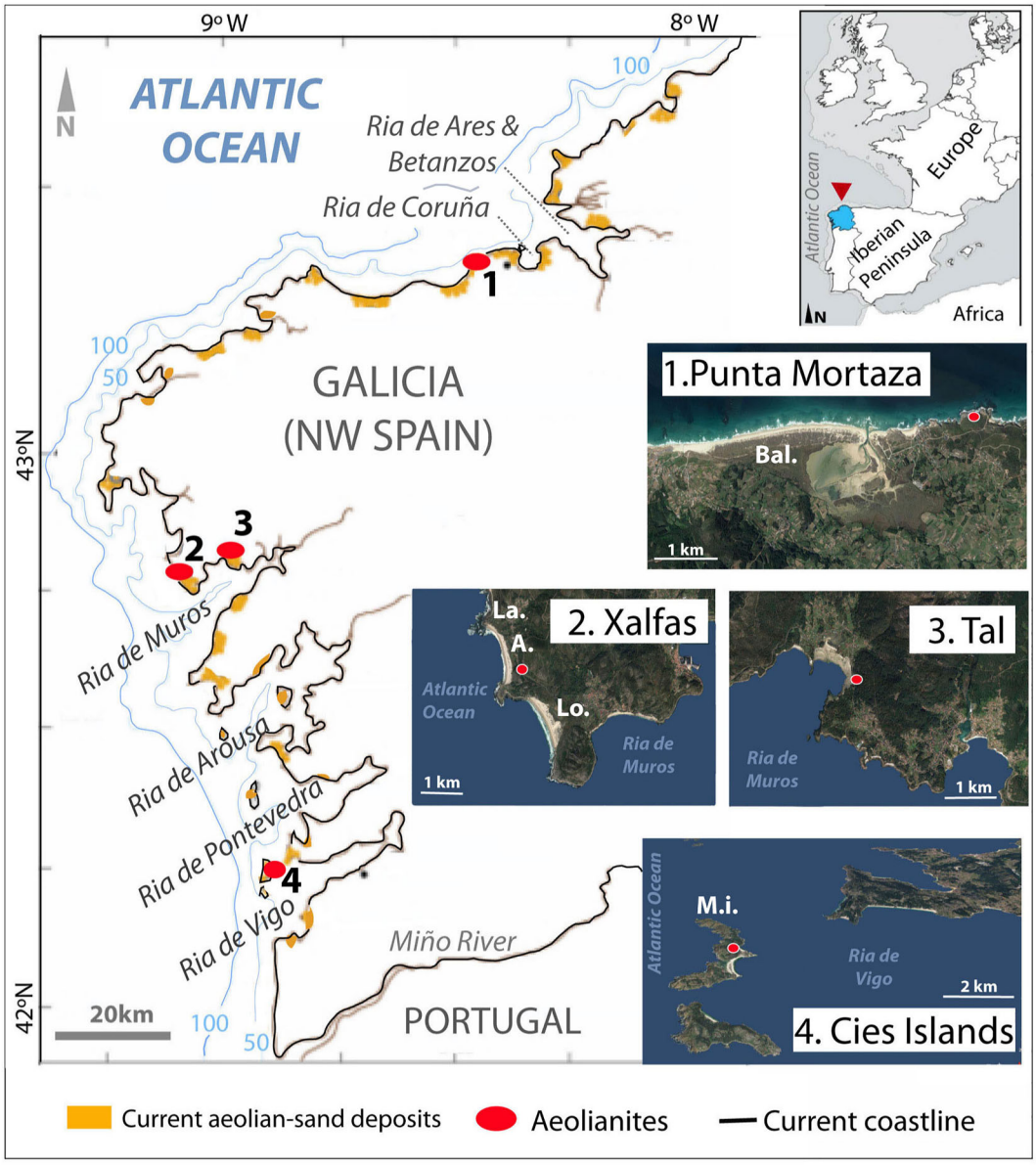


**FIGURE 1** Location of aeolianite outcrops analysed and dated and location of current dune fields and coastal sands on this Atlantic coast. Bal. = Baldaio Beach and dune fields; La. = Lariño; A. = Areamaior Beach; Lo. = Louro Beach; M.i. = Monteagudo Island. [Color figure can be viewed at wileyonlinelibrary.com]

misunderstanding continental deposits (aeolian and/or fluvial) with marine sediments (Cartelle, 2018; Martínez-Carreño et al., 2017; Muñoz-Sobrino et al., 2016). Furthermore, when an aeolian origin has been admitted for coastal sand that today remains totally or partially flooded (Costas et al., 2009; Mohamed et al., 2010), the requirement for extensive emerged areas covered with sand (which can be mobilized by wind) is ignored. Perhaps these are the reasons why coastal dunes are simply considered an extension of sand beaches inland (Ley et al., 2007: 11). This controversial statement assumes that from the sands transported by the sea today (hypothetically) up to the intertidal, in a meso-tidal and cyclic storm regime (Jackson et al., 2019), current aeolian accretion processes are sufficiently intense to form dune ridges in the supratidal area or even inland (which in the study area can exceed 10 m in thickness and cover tens to hundreds of square metres). Such a marine–aeolian sequence of sand transport, which may be consistent with dune formation processes on other types of coast (Engel et al., 2015; Hesp et al., 2021; Jackson et al., 2019), does not fit with the processes observed today on the Atlantic coast of Galicia, where a pronounced erosional character favours the destruction of aeolian sands (Flor-Blanco et al., 2021) as opposed to deposition.

Sedimentary forms that predominate on this coast (excluding fluvial or alluvial deposits) are shingle beaches and sand sediments, which are closely related to Peistocene glacio-eustatic oscillations (Lommertzen, 2011; Viveen et al., 2012). Shingle beach deposits consisting of gravels, pebbles and even large boulders (Figure 2) are present in open coastal areas, where there is significant dissipation of energy produced during big storms. Although the formation of these marine deposits is usually related to erosive processes at the cliff base, shingle beaches frequently appear along the Galician coast on rocky platforms (Figure 2) located at different heights above medium sea level (amsl) and disconnected from any cliff (Lommertzen, 2011; Teixeira, 1949). Their origin has been attributed to erosion of the rocky substrate during brief transgressive maximum episodes (Vidal-Romaní & Grandal-d'Anglade, 2018), taking advantage of the favourable rock structure or reworking of continental deposits (e.g. screes, slope deposits or small alluvial fan debris)—and very rarely due to erosion at the base of the rocky cliff. These types of deposits (Figure 2) include (i) present-day (Holocene postglacial) formations, (ii) dissected deposits between +2 m and +4 m amsl that form a continuum along this Atlantic margin and (iii) older fossil shingle beaches (>350 ky; Trindade et al., 2013) at higher elevations (+15 m amsl).

The sea-level rise during the current interglacial favours the erosion of sand beaches and related dune fields, exposing the most resistant materials on breaking-wave areas (intertidal) such as pebbles and boulders (Vidal-Romaní & Grandal-d'Anglade, 2018). This clearly

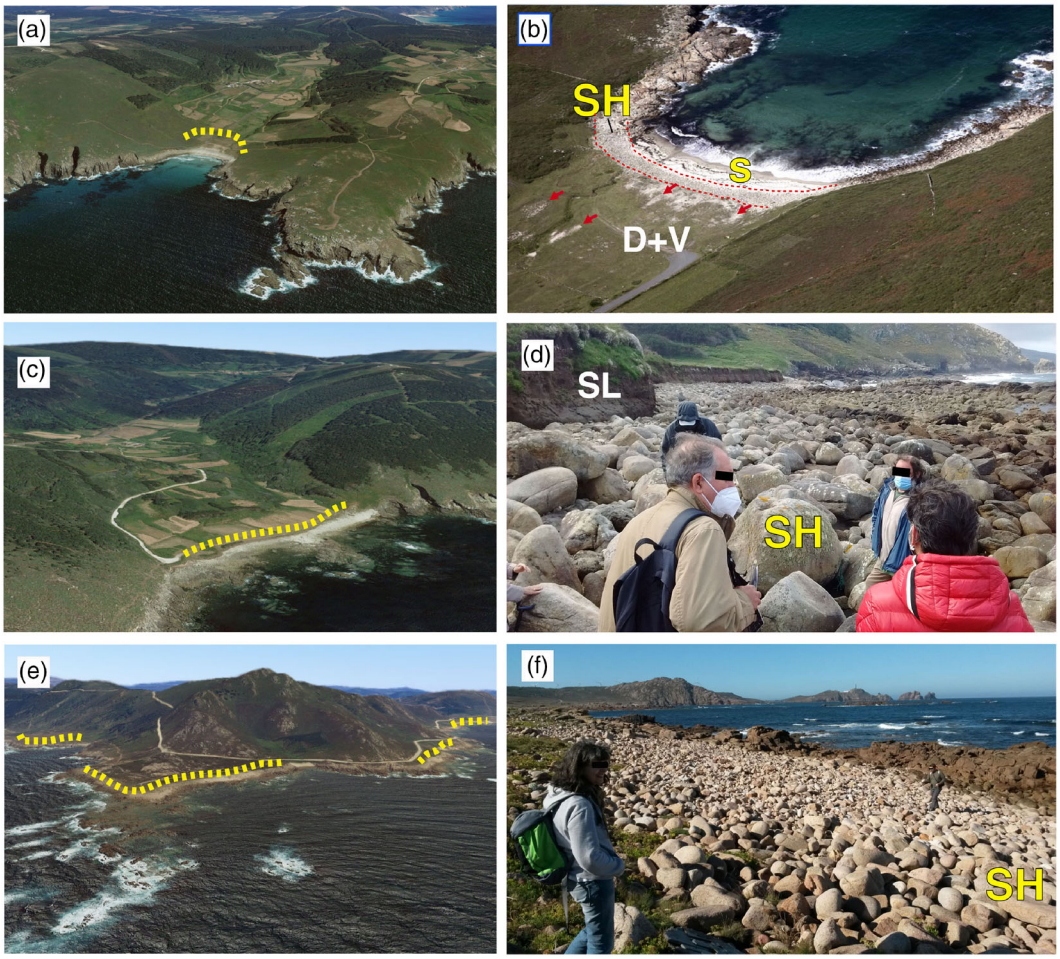


**FIGURE 2** Shingle beaches (yellow dotted line) from Moreiras (a, b; 43°02′N–9°15′W, WGS84), Cuño (c, d; 43°04′N–9°14′W) and Cabo Vilán-Trece (e, f; 43°11′N–9°10′W) (A Coruña, Galicia). SH = shingle beach; S = sands; SL = slope deposits; D + V = dunes covered by terrestrial vegetation. In (b), a red dotted line separates sand/shingle beach/dunes and red arrows indicate erosive blow-out formations. Satellite image ©Google Earth (2020). [Color figure can be viewed at wileyonlinelibrary.com]

indicates a high-energy erosional environment consistent with the formation of shingle beaches, although incompatible with any process of sand sedimentation—beyond a thin cover in the milder seasons (Jackson et al., 2019). In some cases, as shown in Figure 2b, pebbles and boulders from shingle beaches are interspersed between foreshore sands and backshore dune fields. The coexistence of these sedimentary formations of opposite depositional environments suggests the existence of a previous aeolian accretion of sand up to the present coastline, but never simultaneous with the formation of shingle beaches. This makes it necessary to investigate the age and processes that led to the emplacement of sand on the present-day coastline.

## 2 | AEOLIANITE OUTCROPS: ANTECEDENTS

The aeolianite outcrops preserved on the coast of Galicia, as studied here (Figures 1 and 3), have also been observed on the Atlantic coast of Portugal (Gutiérrez-Becker, 2008; Moura et al., 2007) to SW France (Bertran et al., 2020; Bosq et al., 2019). These deposits have been interpreted as fossil aeolian sediments (aeolianites) (Gutiérrez-Becker, 2008; Trindade et al., 2013) and they are preserved both in protected areas in the interior of the rias and in exposed areas of the open coast at heights of up to +45 m or more.

In previous references, the coastal sands of Galicia were erroneously considered as beach deposits and the different height at which they were preserved was used to establish different sea levels (Nonn, 1966). Other authors have interpreted these deposits as marine sands reworked by the wind (Devoy et al., 1996) rather than the opposite. They have also been erroneously considered as marine levels corresponding to a previous interglacial episode (Alonso & Pagés, 2000, 2010; Caraballo-Muziotti, 1969; Gómez-Orellana et al., 2007), although there were already some authors who identified them as aeolian sands (López-Cancelo, 2004; Santos & Vidal-Romaní, 1993), interpreting the aeolianites (Figures 1 and 3) as the remains of sedimentary formations formed and repeatedly destroyed during the glacio-eustatic oscillations of the Quaternary (Nieto & Vidal-Romaní, 1989). At that time, the unavailability of suitable dating techniques did not allow for a more precise chronology.

## 3 | OBJECTIVES

The main objective of this work is to characterize the aeolianite outcrops of Xalfas, Tal, Punta Mortaza and Cíes Islands, as well as to establish their age. These homogeneous and well-sorted sand sediments of siliciclastic materials are suitable for establishing a chronology by extracting an optically stimulated luminescence (OSL) signal from quartz grains. Considering the local sedimentary record, the chronology of these deposits would provide a better understanding of the evolution of coastal dunes in NW Spain, with the aim of their conservation and management.

## 4 | STUDY AREA: AEOLIANITES FROM XALFAS, TAL, PUNTA MORTAZA AND CÍES ISLANDS

The coastline of Galicia (Figure 1), about 2000 km long, is made up of beaches, rocky cliffs and deep embayments called rias. The cliffs, of tectonic origin (De Vicente & Vegas, 2009), define an irregular and steep coastline up to 600 m high. The Galician Rias (Figure 1), on the other hand, are fluvial valleys flooded by the ocean during the present Holocene transgression, giving rise to wide estuaries (Rey-Salgado, 1993) where sedimentation of fine materials predominates (e.g. from sands on beaches or bars, to silts in the bottom of rias and mudflats). Along this coastline, some aeolianite outcrops were also fossilized by slope deposits (Trindade et al., 2013), facilitating their

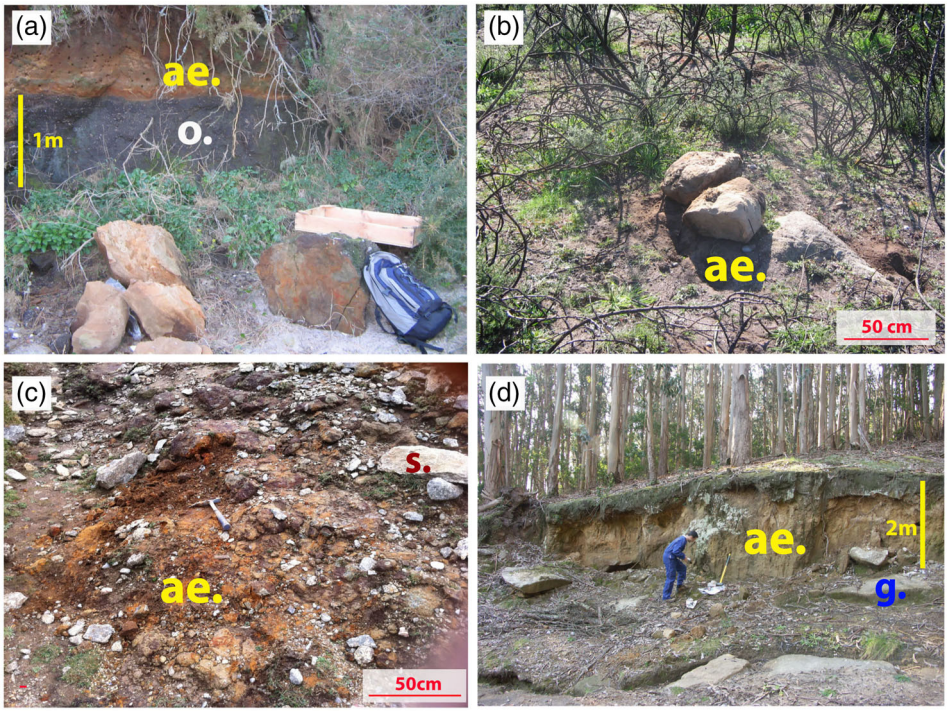


**FIGURE 3** Late Pleistocene aeolianite outcrops in NW Galicia (Spain): (a) Tal; (b) Xalfas; (c) Punta Mortaza; and (d) Cíes Islands. ae. = Aeolian level (aeolianites); o. = organic level; s. = slope deposits; g. = granitic basement. (a) and (b) show brick samples for OSL dating. [Color figure can be viewed at wileyonlinelibrary.com]

preservation as thin (<5 m) siliciclastic wedges. The most representative characteristics of the four aeolianites studied in this work will be described, following their location from north to south on the Atlantic coast of NW Spain. The aeolianite from Punta Mortaza (43°18′26″N; 8°38′43″W, WGS84) (A Coruña, Galicia) is represented by sandy patches less than 1 m thick (Figures 1 and 3c) that are preserved in a very fragmented form on medium cliffs up to 80 m high, on a stretch of open coastline and very close to the extensive sand beach and dune fields of Baldaio. The aeolianite from Xalfas (42°45′43″N; 9°06′23″W) (Figures 1 and 3b) is located on a stretch of open coastline between the Ria de Muros and Lariño. This outcrop reaches heights of +45 m amsl at the base of a spur 300 m above sea level and 600 m away from the present coastline, where a continental lagoon beach system (Lagoa de Xalfas) and extensive sandy areas develop—such as the beach of Louro and Areamaior (Lariño). The Xalfas outcrop shows discontinuous patches of aeolian sand along the rocky platform, very compact and less than 1 m thick (Figure 3b). Below this aeolian level, a basal marine level of about 30 cm appears, represented by quartz and granite pebbles. Occasionally, along the platform, slope deposits overlie the sand deposits. The aeolianite from Tal (Muros, A Coruña) is located in the interior of the Ria de Muros (42°47′16″N; 9°00′55″W) (Figure 1). This outcrop overlies a rocky substrate on which a marine level of pebbles ~50 cm lies at +1 m amsl. The next 2 m are represented by a silty deposit, rich in organic matter (Figure 3a). This is followed by the sandy level studied, reaching thicknesses of up to 2 m, on which an organic horizon less than 0.2 m thick develops. Finally, the Alto da Figueira aeolianite (42°13′45″N, 8°54′15″W) is located in the current Cíes Islands archipelago, at the mouth of the Ria de Vigo (Pontevedra), reaching at least to heights of +40 m amsl on the more protected eastern slope of the Monteagudo Island (Figures 1 and 3d). This aeolianite outcrop develops on the granitic basement and is currently covered by arboreal vegetation.

## 5 | MATERIALS AND METHODS

### 5.1 | Grain size, morphology and microscopic analysis

Grain size analysis was carried out by dry sieving of the raw sample (10 g). The proportion of particle sizes below 500 μm was estimated by laser particle size analysis (Saturn DigiSizer II). The fractions were classified according to Wentworth (1922). Morphological analysis was determined from the roughness and sphericity classes of Powers (1953) by observing 50 quartz grains from the most representative sand fractions of the sample under binocular microscopy. This information was complemented with an analysis of the surface of the most representative quartz grains of the samples and in better preservation conditions by scanning electron microscopy (SEM) (JEOL model JAM-6400) by secondary electrons detection (25 kV), following the surface texture criteria of Torcal-Sainz and Tello-Ripa (1992). Vacuum Au metallization (0.05 mBa) of the cleaned and dehydrated samples was carried out by cathodic electrospray (Sputter Coater) (BAL-TEC SCD004). Associated with the SEM, the semi-quantitative composition of the observed grains was determined by X-ray microanalysis.

### 5.2 | OSL sampling, equivalent dose ($D_e$) and dose rate ($D_r$)

OSL sampling was done by cutting 50 $cm^3$ blocks (Figures 3a and b) for samples of Punta Mortaza, Tal and Xalfas and hammering one steel core for the Cíes outcrop (Figure 3d). In the Luminescence Laboratory of the University of A Coruña, under subdued red light, the outer part of the blocks and cores was removed and the central part dried and sieved for quartz purification. Coarse sand grains (180–250 μm) were treated with HCl and $H_2O_2$ to remove carbonates and organic matter, respectively. Feldspars and heavy minerals were removed by density separation with sodium polytungstate solutions (densities of 2.62 and 2.70 $g/cm^3$) and the obtained quartz was etched in concentrated hydrofluoric acid (40%) to remove any remaining feldspars. This etching removed ~10% of the beta dose rate (Brennan, 2003). The quartz grains were checked with infrared (IR) stimulation to ensure the absence of minerals other than quartz. Luminescence measurements were performed on multigrain aliquots (2 mm in diameter) mounted on stainless steel discs in a Riso-DA15 automated TL/OSL reader equipped with blue light-emitting diodes (LEDs) (470 ± 30 nm) for stimulation and a 9235QA photomultiplier. A Hoya U-340 filter was placed between the photomultiplier and the samples. To irradiate the samples, beta doses were used, with a $^{90}Sr/^{90}Y$ source which provided a dose rate of 0.120 ± 0.003 Gy/s. To estimate the equivalent doses ($D_e$), the single-aliquot regenerative dose (SAR) protocol was used after performing preheat tests and recovery tests were carried out (Murray & Wintle, 2000). The last 4 s of decay curve was subtracted from the fast component (first 0.4 s) to determine the OSL signal (Banerjee et al., 2000).

The dose rate ($D_r$) was estimated using low-background gamma spectrometry on bulk samples. Marinelli beakers were used and measurements were taken in a coaxial Camberra-XTRA gamma detector (Ge-Intrinsic) model GR6022 within a 10 cm-thick lead shield. Guérin's conversion factors were used (Guérin et al., 2011). The alpha contribution was neglected for quartz dose rates, the beta dose rate being corrected due to the HF etching step. Water content and water saturation values were assessed in the laboratory for all samples to estimate an average water content and the cosmic dose rates were calculated in accordance with Prescott and Hutton (1994).

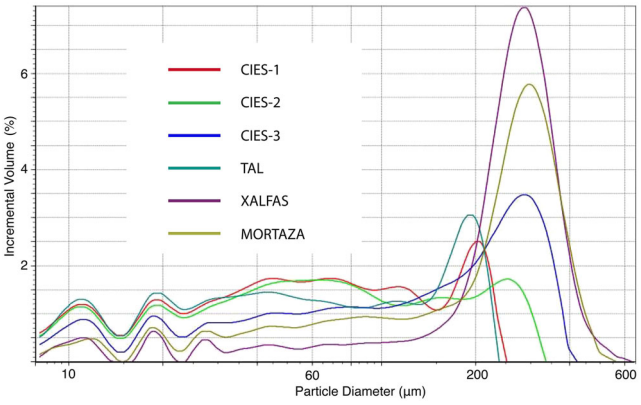


**FIGURE 4** Particle diameter and proportion (%) analysed by laser granulometry (<500 μm) and dry sieving (500–2000 μm) of the samples studied in the aeolianite outcrop of Cíes (Cies-1,2,3), Tal, Xalfas and Punta Mortaza (Mortaza). [Color figure can be viewed at wileyonlinelibrary.com]

## 6 | RESULTS

### 6.1 | Granulometric, morphoscopic and microscopic analysis

The major grain size fractions by dry sieving are fine and medium sands. However, laser granulometry (Figure 4) shows that in some samples there is a similar proportion of silt. The sample from Punta Mortaza shows a high content of quartz grains, good sorting and ochre colouration (iron oxides) (Figures 3a, c and d), associated with post-depositional leaching processes. The proportion of sand-sized particles obtained from laser granulometry is 75% of the fine fraction (<63 m). The morphology of the sand grains is sub-rounded. In the Xalfas sample, 80% of the material corresponds to the fine and medium sand fractions, with sub-angular and sub-rounded morphology. The textural classes of the aeolian level of the Tal sample are represented by 60% silt and 40% sand. The morphology of the quartz grains corresponds to the sub-rounded classes. For the Cíes Islands samples, the proportions are 40% silts and 60% fine-to-medium sands, whose morphology corresponds mostly to the sub-rounded classes.

Microscopic analysis (SEM) (Figure 5) reveals the presence of rough surfaces and impact marks related to aeolian transport (Pye & Tsoar, 1990), such as angular shock v-marks (both polygonal, crescent and other irregular shapes), shock arcs or well-polished hertzian and/or conchoidal fractures (Figure 5).

### 6.2 | OSL dating

#### 6.2.1 | Dose rate

To estimate the $D_r$ (Table 1), a saturation percentage of 5 ± 0.5% was assumed for all the samples. In this material there is an average proportion of fine sand over 50%, so the drainage conditions are favourable, reducing the attenuation of the radiation for content in interstitial water (Guérin & Mercier, 2012). The high grade of homogeneity minimizes the variations related to beta dosimetry (Nathan et al., 2003). Nevertheless, a slight disequilibrium in the $^{238}U$ decay chain in the samples of Xalfas and Punta Mortaza was observed. It has been considered that uranium disequilibrium occurred during the whole burial time of the quartz grains, and secular equilibrium during the burial time, estimating maximum and minimum total $D_r$ values. Both cases were used to estimate an average $D_r$, being the uncertainty of the sum of errors (Arce-Chamorro, 2017). Under secular equilibrium conditions, the total $D_r$ was 3.5 ± 0.3 and 3.6 ± 0.8 Gy/ky for Xalfas and Mortaza, respectively. Under disequilibrium conditions, the total $D_r$ was 1.5 ± 0.1 and 2.9 ± 0.6 Gy/ky for Xalfas and Mortaza, respectively. Corrected values and $D_r$ values for the other samples are summarized in Table 1, ranging between 3.3 and 2.1 Gy/ky. Such $D_r$ is similar to those estimated for other aeolianite outcrops and quartz-rich continental deposits in the region (Arce-Chamorro, 2017; Ribeiro et al., 2019; Viveen et al., 2012).

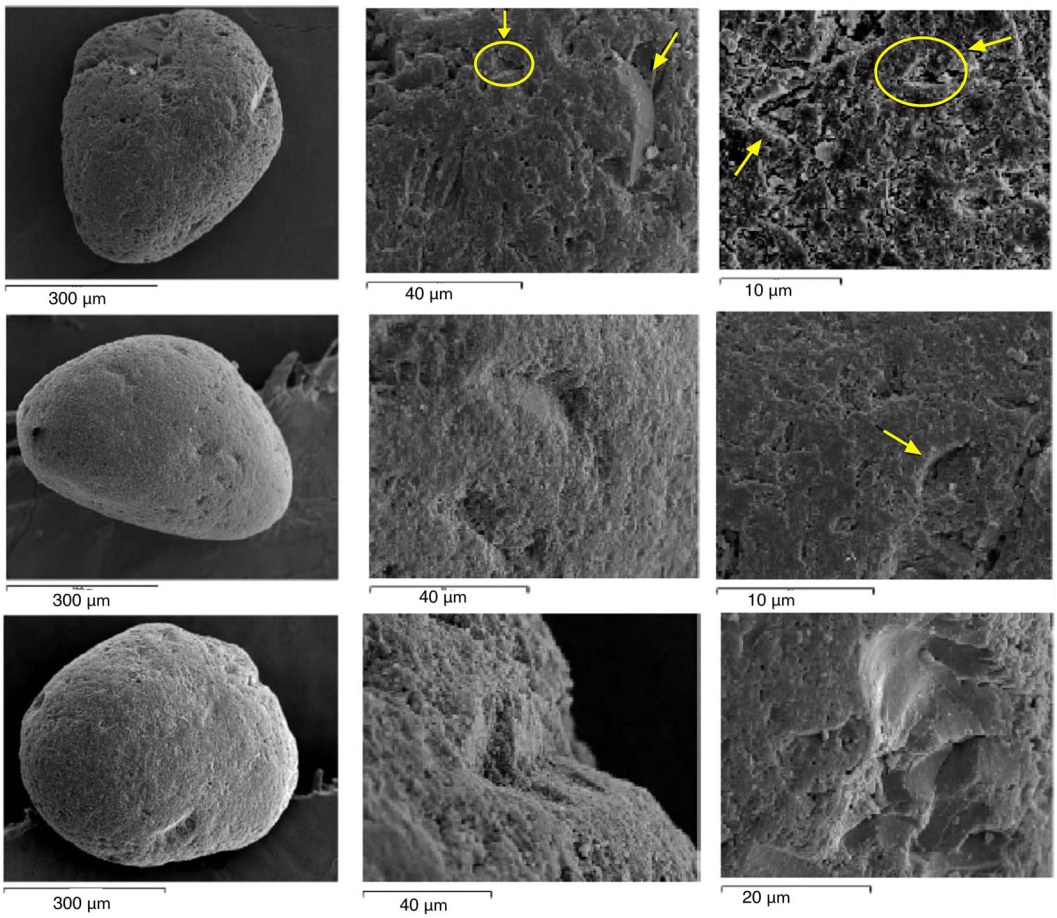


**FIGURE 5** Examples of the most representative aeolian impact marks (as shock v-marks, shock arcs or conchoidal fractures) analysed by SEM on quartz grains from the Tal and Xalfas samples (modified from Gutiérrez-Becker, 2008). [Color figure can be viewed at wileyonlinelibrary.com]

**TABLE 1** Radio-isotopic activity of the series of $^{238}$U and $^{232}$Th, as well as $^{40}$K (Bq/kg), dose rate ($D_r$) (Gy/ky), equivalent dose ($D_e$) (Gy) and OSL ages (ka: kiloannum = kiloyear [ky] = 1000 years before dating). *N* = number of aliquots accepted/analysed; *OD* = overdispersion. $D_r$ from Xalfas and Punta Mortaza corrected due to disequilibrium in the $^{238}$U decay chain

| Sample | $^{238}$U (Bq/kg) | $^{226}$Ra (Bq/kg) | $^{232}$Th (Bq/kg) | $^{40}$K (Bq/kg) | $D_r$ (Gy/ky) | *N* | *OD* (%) | $D_e$ (Gy) | Age (ka) |
|---|---|---|---|---|---|---|---|---|---|
| Xalfas | 183 ± 3.8 | 59 ± 4 | 10 ± 1 | 79 ± 8 | 2.6 ± 1.7 | 31/56 | 50 ± 8 | 53 ± 6 | 20.9 ± 6.5 |
| Punta Mortaza | 68 ± 1.4 | 30 ± 1 | 82 ± 3 | 349 ± 09 | 3.3 ± 0.9 | 29/74 | 22 ± 7 | 94 ± 8 | 29.7 ± 4.8 |
| Tal | 13 ± 4 | 17 ± 1 | 17 ± 1 | 475 ± 45 | 2.1 ± 0.3 | 21/56 | 34 ± 6 | 62 ± 5 | 30.9 ± 3.6 |
| Cies-1[a] | 18 ± 2.4 | 18 ± 2.4 | 20 ± 2.6 | 660 ± 38 | 2.7 ± 0.4 | 31/96 | 20 ± 4 | 80 ± 3 | 30.6 ± 4.8 |
| Cies-2[a] | 27 ± 1.3 | 18 ± 2.1 | 19 ± 2.8 | 570 ± 35 | 2.4 ± 0.3 | 36/54 | 50 ± 6 | 56 ± 5 | 23.3 ± 3.9 |
| Cies-3[a] | 19 ± 1.2 | 15 ± 2.2 | 15 ± 4.8 | 485 ± 31 | 2.1 ± 0.3 | 37/96 | 33 ± 5 | 42 ± 3 | 20.1 ± 3.3 |

[a]Data from Arce-Chamorro (2017), Arce-Chamorro et al. (2021).

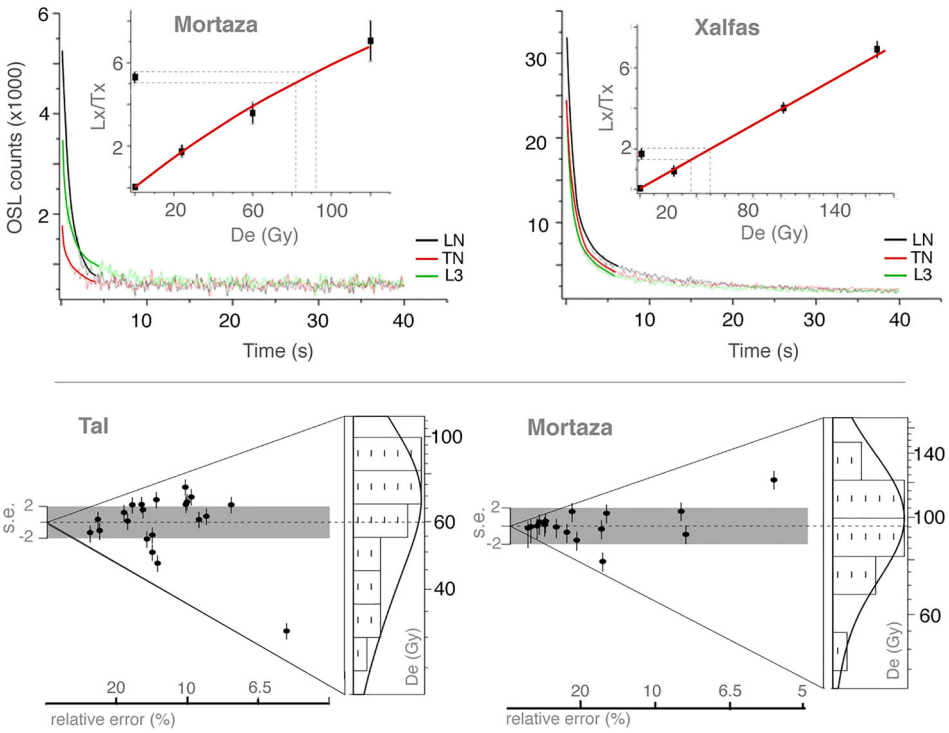


**FIGURE 6** OSL signal decay curve and normalized OSL signal growth curve for Punta Mortaza (Mortaza) and Xalfas samples. Equivalent dose ($D_e$) distributions by abanico plots (Burow et al., 2016) of the Tal and Punta Mortaza (Mortaza) samples. [Color figure can be viewed at wileyonlinelibrary.com]

### 6.2.2 | OSL signal, $D_e$ and age estimation

All aliquots exceeding the SAR acceptance criteria show fast decay curves, either for the natural OSL signal, the natural test-dose signal or any of the regenerated OSL signals (Arce-Chamorro, 2017), with more than 90% of the signal being recorded during 1 s of blue-light stimulus. The luminescence sensitivity of the materials analysed is variable. A high proportion of aliquots had low natural OSL signal intensity (<20 000 counts/unit of time [c/ut]), low normalization ratios (<10) and an associated error between 5 and 20%, increasing with dose (Figure 6). A small number of more sensitive aliquots were also observed, with a higher natural OSL signal (>50 000 c/ut), high normalization ratios (>10), an associated error below 15% and estimates of equivalent dose ($D_e$) close to central statistical estimators (Arce-Chamorro, 2017), such as the median, arithmetic mean and error-weighted mean of the central age model (CAM) (Galbraith et al., 1999). Such differences in the quartz signal could justify the wide dispersion observed in the distributions of the $D_e$ of each aliquot (Figure 6) and the high percentage of overdispersion (*OD*) with respect to the central dose of the CAM, between 20 and 50% (Table 1).

## 7 | DISCUSSION

### 7.1 | Aeolian sands and OSL dating

The grain size estimated by laser granulometry fits well with the expected grain size of aeolian sediments (Vandenberghe, 2013), as well as sphericity and roundness and impact marks observed by microscopy. The absence of both foraminifera and saltwater diatoms agrees with such features, and all of them clearly show an aeolian origin (Gutiérrez-Becker, 2008). The studied aeolianites of Xalfas and Cíes-Alto da Figueira reach heights of +40 m amsl without original sedimentary structures, indicating that they are climbing dunes (Greeley & Iversen, 1985; Hay et al., 2021; Pye & Tsoar, 1990; Tyson, 1999). OSL data showed no evidence of incomplete signal bleaching, and so complete exposure to sunlight, unlike can be observed for other aeolian materials such as loess. This reduces the probability of overestimation of the $D_e$ and age (Jacobs, 2008). As mentioned above, the measured aliquots show a high dispersion but symmetric distributions and good fit to normal distributions. Thus, the CAM was used to assess the $D_e$. The obtained $D_e$ is summarized in

**TABLE 2** Results of $^{14}$C AMS dating of some selected samples. $^{14}$C age calibrated with OxCal 4.4 (Bronk-Ramsey, 2009) with the calibration curve IntCal20 (Reimer et al., 2020). Locations from north to south. Height in metres (m) above (+) or below (−) medium sea level at present day

| NW Iberian coast | Formation | Height (m) | $^{14}$C AMS age (BP) | Intcal-20 cal yr (BP) | Material | Reference |
|---|---|---|---|---|---|---|
| Arealonga Beach I (Lugo) | Submerged forest | +1 | 3080 ± 30 | 3370–3212 | Red deer bones | Vidal-Romaní and Grandal-d'Anglade (2018) |
| Arealonga Beach II (Foz/Lugo) | Heathland | +1 | >40 000 | >40 000 | Wood | Gómez-Orellana et al. (2007) |
| Doniños Beach (A Coruña) | Freshwater lagoon | −6 | 1795 ± 75 | 1874–1533 | Organic sediment | López-Cancelo (2004) |
| | | −7 | 7315 ± 25 | 8177–8033 | Pollen-enriched extract | Sáez et al. (2018) |
| | Submerged forest | −7 | 9020 ± 25 | 10 237–10 180 | Carbonized root | |
| Ponzos Beach (A Coruña) | Submerged forest | −0.5 | 5860 ± 40 | 6785–6559 | Wood | Gómez-Orellana et al. (2021) |
| | | −1.4 | 6720 ± 40 | 7668–7510 | Organic sediment | |
| Seselle Beach, Ria de Ares (A Coruña) | Freshwater lagoon | 0 | 3450 ± 100 | 3971–3463 | Wood | Santos and Vidal-Romaní (1993) |
| | | −0.7 | 4350 ± 90 | 5296–4653 | Organic matter | |
| | Submerged forest | +1 | 4190 ± 30 | 4840–4589 | Horse bones | Vidal-Romaní and Grandal-d'Anglade (2018) |
| Ria de Coruña (A Coruña) | Submerged forest | +1 | 3925 ± 45 | 4518–4187 | Wood | López-Cancelo (2004) |
| Traba Beach (A Coruña) | Freshwater lagoon | −4 | 3780 ± 50 | 4383–3983 | Organic sediment | Bao et al. (2007) |
| Ria de Muros | Freshwater lagoon | +2 | 24 060 ± 360 | 29 091–27 669 | Organic sediment | Gutiérrez-Becker (2008) |
| Louro Beach (A Coruña) | Freshwater lagoon | −2 | 7170 ± 30 | 8024–7936 | Organic sediment | González-Villanueva et al. (2015) |
| Areoso Islet, Ria de Arousa (Pontevedra) | Submerged forest | −1 | No data* | 3865–3695* | Wood | Blanco-Chao et al. (2017) |
| | Submerged forest | −1 | No data* | 3407–3249* | Terrestrial vegetation | Cajade-Pascual et al. (2019) |
| Southern Continental Shelf | Aeolian sands | −100 | 18 010 ± 90 | 22 186–21 466 | Mixed foraminifera | Mohamed et al. (2010) |
| Cíes Islands, Ria de Vigo (Pontevedra) | Aeolian sands | −2 | 21 680 ± 60 | 26 030–25 835 | Organic sediment | Costas et al. (2009) |
| | | | 17 240 ± 50 | 20 933–20 604 | Organic sediment | |
| | | −1 | 3750 ± 30 | 4233–3916 | Organic sediment | |
| | Sands with dune vegetation | −5 | 5850 ± 30 | 6744–6561 | Bioclasts (shell fragments) | Muñoz-Sobrino et al. (2016) |
| Ria de Vigo | Sandy silts (freshwater) | −35 | 39 890 ± 440 | 44 086–42 628 | Bryophyte | Martínez-Carreño and García-Gil (2017) |
| North Portugal coast | Submerged forest | +1 | 5880 ± 60 | 6853–6502 | Wood | Ribeiro et al. (2011) |
| Central-North Portugal coast | Submerged forest | +1 | 24 500 ± 260 | 29 212–27 998 | Wood | García-Amorena et al. (2007) |

*No $^{14}$C AMS data; calibrated age by Intcal-13.

Table 1. The estimated errors are below 11%. Tal and Punta Mortaza samples exhibited *OD* values (Table 1) within the expected limit for well-bleached samples (30%) (Galbraith & Roberts, 2012). For the Xalfas sample, despite having an *OD* of 50%, the CAM provides an age that agrees with both the Tal and Punta Mortaza sample ages. Indeed, the CAM is commonly used when similar *OD* values are observed in the literature for samples without incomplete bleaching (Bickel et al., 2015; Hardt et al., 2016; Muñoz-Salinas et al., 2017; Trauerstein et al., 2014). The obtained ages are 20 ± 6 ky for the Xalfas sample, 29 ± 4 ky for Punta Mortaza and 30 ± 3 ky for the Tal sample. The calculated OSL burial-age range for Tal is consistent with the underlying continental lagoon deposit (Figure 3a) dated by radiocarbon, back to 29 ± 0.5 ky cal BP (Gutiérrez-Becker, 2008) (Table 2). The burial ages estimated for the aeolianites from Cíes Islands (Table 1) are chronologically consistent.

## 7.2 | Coastal aeolianite outcrops: Chronology and sedimentary implications

In recent years, thanks to the use of absolute dating techniques such as OSL (Arce-Chamorro, 2017; Ribeiro et al., 2019; Trindade et al., 2013; Viveen et al., 2012), it has been possible to establish a reliable age of formation for siliciclastic deposits on the Atlantic coast of Galicia. The aeolianite from Cíes Islands has been dated back between 30 and 20 ky (Figure 7). In such period the sea level was −120 m below medium sea level (bmsl) (Waelbroeck et al., 2002) and the islands were fully connected to the mainland (Arce-Chamorro et al., 2021). Other 20 ky-old aeolian sands have been identified on the nearest continental shelf (Mohamed et al., 2010) at −100 m bmsl, as well as the 20 ky-old partially flooded dunes preserved today in the Cíes Islands (Costas et al., 2009) (Table 2). Thus, the obtained chronology for three aeolianites preserved at different points of the Galician coast (Xalfas, Tal and Punta Mortaza), between 30 and 20 ky (Table 1, Figure 7), is in good agreement with the model of evolution of the Galician coast during the Holocene transgression previously proposed by Vidal-Romaní and Grandal-d'Anglade (2018). This aeolian accretion at the end of MIS2 is also represented on the northern coast of Portugal by dunes dated back from 30 to 12 ky old (Costas et al., 2012; Thomas et al., 2006).

The aeolian processes were active from the end of the last glacial episode (MIS2) (Lisiecki & Raymo, 2005; Petit et al., 1999) with a local sea level of −120 m bmsl (Arce-Chamorro et al., 2021; Mohamed et al., 2010) (Figures 7 and 8). At that time, the aeolian sands were placed up to the areas that define the present-day coastline. This regressive level implied a shoreline shifted down to 20 km (Arce-Chamorro et al., 2021), resulting in the subaerial exposure of a wide strip of the continental shelf (Figure 8) covered with sand and silt sediments up to 20 m thick (Rey-Salgado, 1993) and even more. Assuming similar wind dynamics to present (Figure 8), the sand would be easily transported through the continental shelf (EMODnet, 2018; Rey-Salgado, 1993) with no other limitation than the most active fluvial channels (Figure 8).

Subsequently, as the sea level rose during the Holocene transgression, the transport of aeolian sands continued, despite the sand supply being reduced by the progressive flooding of the source area (the continental shelf). There are numerous examples related to freshwater lagoons (Table 2) dating back to 15 and 10 ky (Sáez et al., 2018), 8 and 4 ky (Bao et al., 2007; Costas et al., 2009; González-Villanueva et al., 2015; Sáez et al., 2018; Santos & Vidal-Romaní, 1993). This continued aeolian accretion explains the growth of Holocene climbing dunes, covering steep reliefs of more than 200 m in altitude at the time of their formation, such as the climbing dune of the Cíes Islands mentioned above. This would be the case, among many, of the relict climbing dunes still preserved on the NW coast of Spain, such as the one at Trece or Ponteceso (A Coruña) (Figure 9), reaching heights of over +150 m amsl. The OSL dating of these climbing dunes is currently in progress, yielding minimum formation ages of 5 ky (Pardiñas-González, 2021), thus fitting the innovative model proposed here.

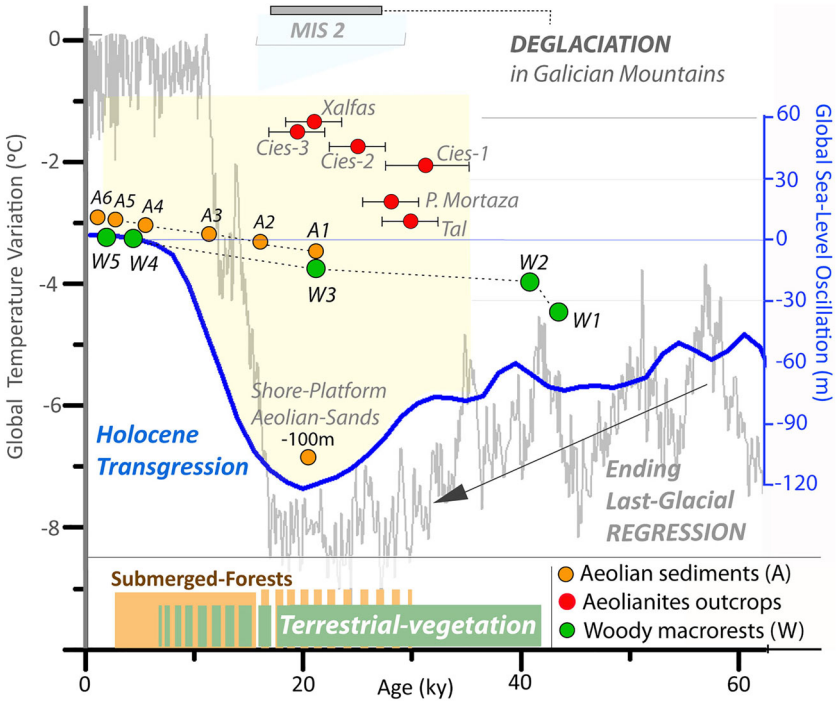


**FIGURE 7** Temperature variations from Vostok ice cores (Petit et al., 1999) (grey line) and sea-level oscillations (Waelbroeck et al., 2002) (blue line) for the last 60 ky, including deglaciation processes in inland Galicia and northern Portugal (Vidal-Romaní et al., 2015) at MIS2. −100 m bmsl aeolian sands (Mohamed et al., 2010). (A) Aeolian sediments. A1 = Cíes Islands (Costas et al., 2009); A2 = Doniños Beach (Sáez et al., 2018); A3 = Northern Portugal (Costas et al., 2012); A4 = Seselle Beach (Santos & Vidal-Romaní, 1993; A5 = Cíes Islands (Costas et al., 2009); A6 = Areoso Islet (López-Romero et al., 2020). (W) Woody remains and submerged forest. W1, W2 = Ria de Vigo (Martínez-Carreño & García-Gil, 2017; W3 = Cíes Islands (Costas et al., 2009); W4 = Ria de Coruña (López-Cancelo, 2004); W5 = Areoso Islet at ria de Arousa (Blanco-Chao et al., 2017). [Color figure can be viewed at wileyonlinelibrary.com]

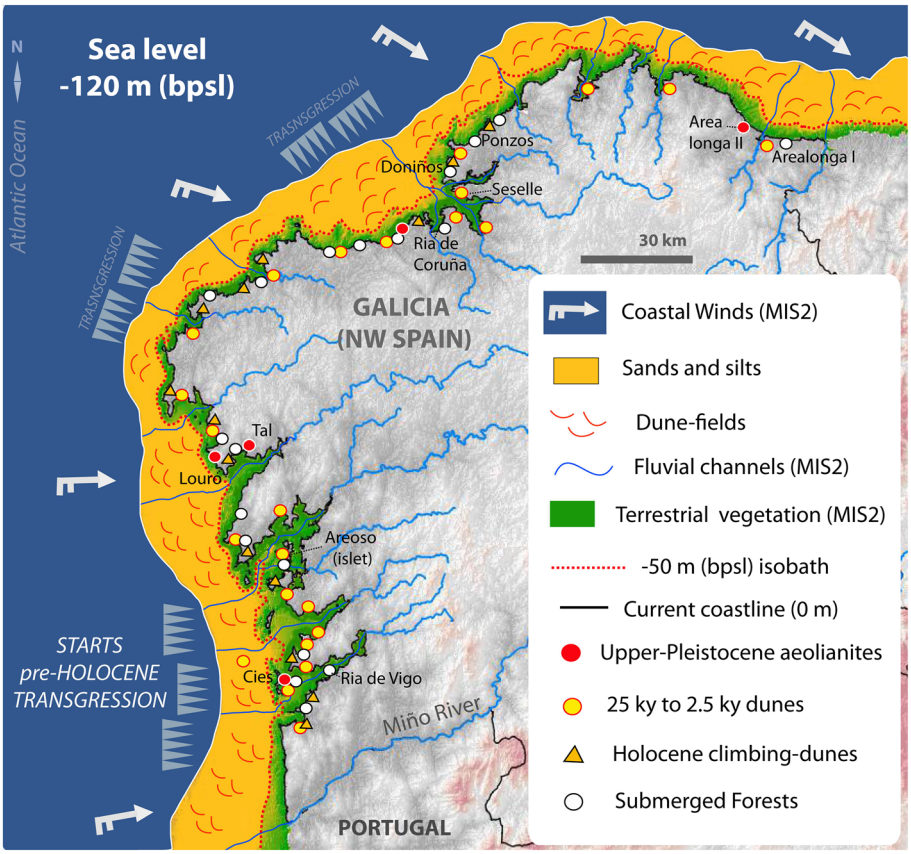


**FIGURE 8** Mobilization of the dune fields by coastal winds (white arrows) from the emerged continental shelf towards the continent, with a sea level of −120 m (bmsl) 20 ky ago, giving rise to the Upper-Pleistocene aeolianites (red dots). At this moment the fluvial valleys were covered by terrestrial vegetation (green area), as well-developed forests. As the sea level rose progressively from the beginning of the last interglacial transgression and reached the −50 m (bmsl) isobath (dotted red line), the pre-Holocene and Holocene aeolian formations (yellow dots) and Holocene climbing dunes (orange triangles) grew and reached the current coastline (black line). From this moment on the coastal environments were buried by dune fields, as the submerged forest (white dots) suggests. Bathymetry (EMODnet, 2018); DEM srtm90 (NASA, 2000). [Color figure can be viewed at wileyonlinelibrary.com]

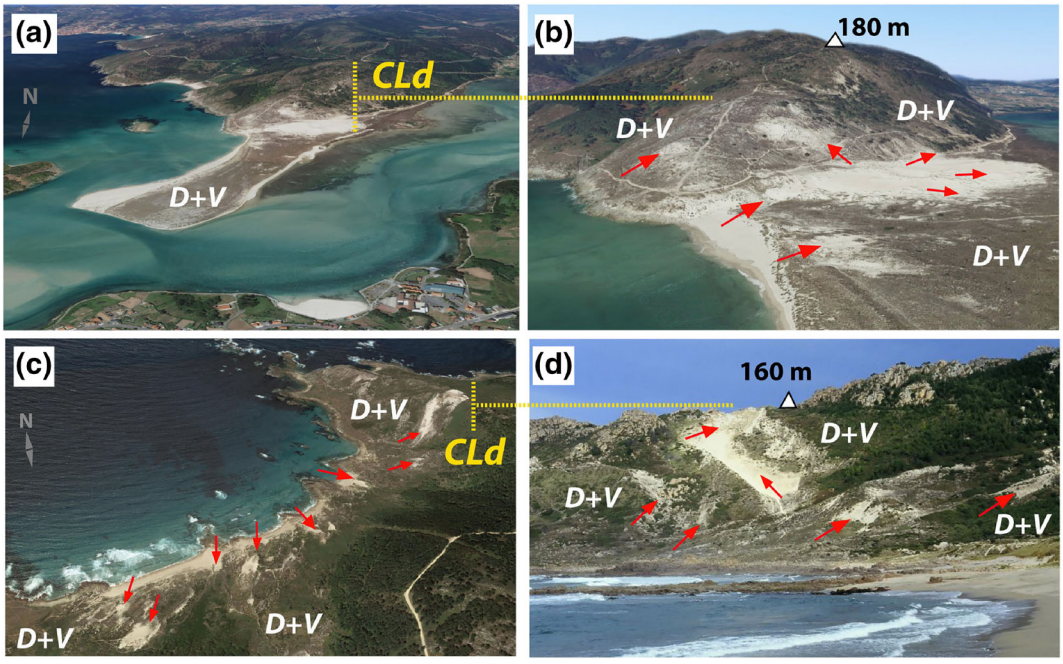


**FIGURE 9** (a, b) Climbing dune (CLd) from Ponteceso (A Coruña; 43°14′N–8°56′W, WGS84). (c, d) Climbing dune from Trece Beach (A Coruña; 43°11′N–9°08′W). D + V = dunes and vegetation. Note the vegetation now covering all relic aeolian sands (as dunes and climbing dunes) and the blow-out formations (red arrows) eroded by coastal winds during storms. Satellite image ©Google Earth (NASA, 2000). [Color figure can be viewed at wileyonlinelibrary.com]

This model also explains the origin of present-day sand beaches. As mentioned, sand beaches were previously considered only as marine sediments reworked by wind (Devoy et al., 1996), based on the distribution of materials transported by rivers to the sea and their subsequent redistribution along the coast by marine currents (Dias et al., 2002). However, this redistribution, which may occur on other coasts, is not observed in this coastline of cliffs and wide estuaries (rias). According to previous studies on the Atlantic coast of Galicia, the sands are deposited at the mouth of the rivers and/or in the innermost areas of the estuaries where the deposition of fine materials

(e.g. silts in the marshes) prevails (García-Moreiras et al., 2019; Nombela & Vilas, 1987; Rey-Salgado, 1993). Conversely, these fluvial sands never reach the open coast (Oberle et al., 2014; Rosón et al., 2008). In addition, there is no evidence of the transport of suspended sands or silts by marine currents to the coast from the more abundant rivers further south that do not form rias (such as the Miño, Lima or Douro rivers) (Oberle et al., 2014), although this is the general assumption to explain the presence of silts and sands on the bottom of the shelf (Dias et al., 2002). In contrast, the continued aeolian accretion that emplaced the dunes on the current coastline since the end of MIS2, as proposed here (Figures 7 and 8), suggests that sand beaches are aeolian sands that were swept by waves and reworked by tides as the sea reached its present-day level in the Late Holocene. Thus, the upward migration of the sea level formed new beaches where there were dune fields and, in addition, left behind flooded dunes (Cawthra et al., 2022). This is also evidenced by the grain size analyses of the flooded sands from the inner shelf (Pazos et al., 1997), where aeolian impact marks has also been observed in the quartz grains. The general absence of well-developed foraminiferal associations in the studied drilling cores (Cartelle, 2018; Costas et al., 2009; González-Villanueva et al., 2015; Martínez-Carreño & García-Gil, 2013, 2017; Muñoz-Sobrino et al., 2016; Santos & Vidal-Romaní, 1993) also indicates an aeolian origin for most coastal sands in this area. Other revealing evidence is the presence of wind-sorted foraminiferal remains, with aeolian polishing marks, rounded shapes and small size selection (López-Cancelo, 2004) in these sand sediments of aeolian origin. There is other indirect evidence such as the submerged forests (Figure 10) that appear underlying sand beaches, which implies the mobilization of large dune fields capable of burying well-developed tree formations, as will be discussed later (see Section 7.2.2). Subsequent flooding and/or marine reworking of aeolian sands would favourably explain the presence of salt crusts and polished surfaces on the quartz grains from fine and medium sands (Pazos et al., 1997) or the presence of neoformation marine minerals related to shallow environments such as glauconite (Martínez-Carreño et al., 2017).

### 7.2.1 | Continental environments, submerged forests and coastal dunes

A sea level of about −120 m bmsl (Arce-Chamorro et al., 2021; Mohamed et al., 2010) at the end of MIS2 (Figure 8) favoured the development of continental ecosystems in the lowermost areas of the fluvial valleys that today remain flooded by the sea, resulting in the growth of dense forests (Vidal-Romaní & Grandal-d'Anglade, 2018).


**FIGURE 10** Fossilized tree trunks and roots in living position at (a) North Portugal (García-Amorena et al., 2007), (b) Amble, Northumberland (UK), (c) Ceredigion, Mid-Wales, (d) Galway Bay, Ireland (Williams & Doyle, 2014), and (e, f) A Coruña, Galicia (Vidal-Romaní & Grandal-d'Anglade, 2018). SH = shingle beach; FS = forest soil; TR = tree root remains (in their life position); D + V = dunes covered by vegetation. [Color figure can be viewed at wileyonlinelibrary.com]

On the northern coast of Galicia, heaths of more than 40 ky have been identified at +2 m amsl (Gómez-Orellana et al., 2007). The local submerged record from the southern coast (Ria de Vigo) includes organic levels of 42 ky cal BP at −35 and −20 m bmsl, with macrofossils of terrestrial vegetation (see MRV3 and B5 cores in Martínez-Carreño & García-Gil, 2017) (Table 2). Costas et al. (2009) also identified macrofossils of terrestrial vegetation in organic levels interspersed between sand dunes of more than 20 ky cal BP in the Cíes Islands (Table 2) as a natural boundary of more than 300 m high at that time (Arce-Chamorro et al., 2021) between the Galician continental shelf and the Ria de Vigo (Figure 8). This would already indicate that the continental environments on this coast were affected by dunes. This hypothesis is supported by the submerged forests that appear under the intertidal sands of aeolian origin during storm events, along the coast of Galicia and North-Central Portugal (García-Amorena et al., 2007; Gómez-Orellana et al., 2014; Granja & Soares de Carvalho, 1995; Ribeiro et al., 2011; Vidal-Romaní & Grandal-d'Anglade, 2018) (Table 2, Figure 11), as well as the French Atlantic coast and southern British Isles (Bicket & Tizzard, 2015; Westley & Woodman, 2020; Williams & Doyle, 2014) (Figure 10). This highlights the regional importance of this aeolian accretion model.

Galician submerged forests are classified as temperate and deciduous forests, as deduced from the isotopic analysis of the macrofaunal bone remains included among the plant macrofossils (Vidal-Romaní & Grandal-d'Anglade, 2018) (Table 2), and they were in full development until 3.5 ky ago (Muñoz-Sobrino et al., 2016; Nombela et al., 2005; Santos & Vidal-Romaní, 1993) (Table 2) with a sea level lower than the present one. According to this cumulative aeolization model, the mobilization of dune fields from the shelf towards the continent covered a large part of these coastal forests from the end of MIS2 to the Late Holocene. Subsequently, the sea-level rise to present-day levels has led to the flooding/reworking/marine erosion of the aeolian sands, favouring the sporadic and brief appearance of the submerged forests in the present intertidal (Vidal-Romaní & Grandal-d'Anglade, 2018). The erroneous interpretation of coastal sands as present-day marine formations (Alonso & Pagés, 2010; Gómez-Orellana et al., 2007, 2014) ignores the most logical sequence of aeolian accretion. This is the case of the 7 ky woody macrofossils found on the north coast of Galicia (Table 2), subjectively interpreted as materials removed from the seabed and moved by the waves to the intertidal (see figure 2 of Gómez-Orellana et al., 2021), although they are represented by fossil roots and trunks in a living position (Figure 10). It is the waves stirring up the sands that uncover all these macrofossils and even the organic soil of the palaeo-forest (Vidal-Romaní & Grandal-d'Anglade, 2018), some of them buried by aeolian sands 25 ky ago (García-Amorena et al., 2007; Granja & Soares de Carvalho, 1995) (Table 2, Figure 10) when the sea level was at −120 m bmsl (Waelbroeck et al., 2002) and the coastline was

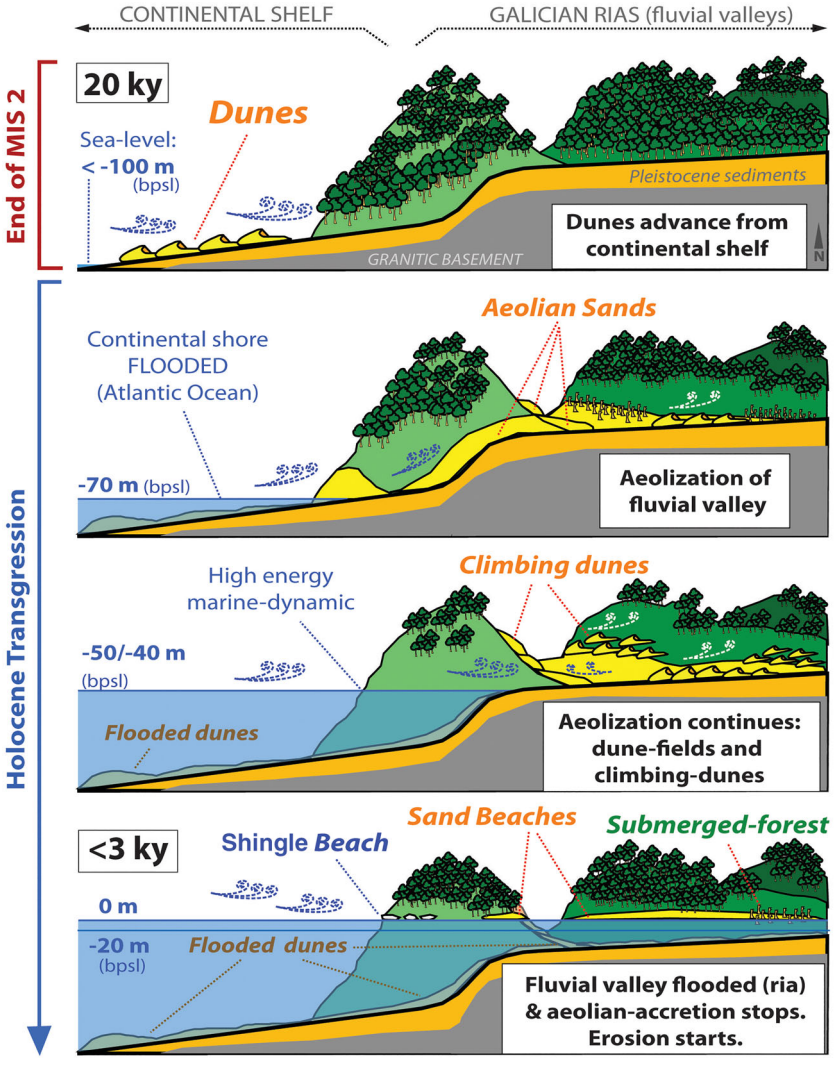


**FIGURE 11** Hypothetic mobilization of sands from the continental shelf (aeolian source area) with sea level below −100 m (bmsl) 20 ky ago. The dunes overcame steep reliefs (climbing dunes) and buried the forested formations at the end of the last regressive episode up to the Early and Middle Holocene (transgression). Flooding of both the lowermost areas of the fluvial valleys and the dune fields less than 3 ky ago led to the Galician rias. At this moment, the waves swept the dunes and formed the present-day sand beaches. Today, the waves stir up the relic (aeolian) sands of the intertidal zone, bringing out the old shingle beaches and submerged forests. [Color figure can be viewed at wileyonlinelibrary.com]

displaced more than 20 km to the west (Figure 7). As can be observed, this pattern is repeated along the entire southern half of the European Atlantic coast.

Comparatively, dune fields on the Atlantic coast of Portugal (Loureiro et al., 2012; Vousdoukas et al., 2012) and SW Spain (Gracia et al., 2006; Ley et al., 2007; Muñoz-Vallés & Cambrollé, 2014) are more extensive than the relict dunes of NW Spain. According to the model proposed here, this would be due to the existence of a larger continental shelf and a larger amount of supply (sands on the emerged shelf) at the time of their formation—as suggested in the Aquitaine Basin (SW France) (Bertran et al., 2020). Chronologically, the model would also be applicable to the entire Atlantic coast of SW France, the Iberian Peninsula and Gibraltar, since the formation of coastal dunes had continuity from the end of the last glacial period (MIS2) to the Late Holocene, as indicated by OSL and radiocarbon dating (Costas et al., 2012; Leira et al., 2019; Rodríguez-Vidal et al., 2004, 2014; Salvany et al., 2011; Sitzia et al., 2015; Zazo et al., 2005). This interpretation would also be valid for the fossil dunes previously identified on the Atlantic coast of the Canary Islands (Vidal-Romaní et al. in IGME, 2004) and recently dated between 30 and 15 ky (Roettig et al., 2017).

### 7.2.2 | Culmination of the aeolian accretion process

The process of aeolian accretion on the Galician coast also continued during the Late Holocene (Figure 11), as suggested by the partially flooded dunes on the current Areoso Islet (in the interior of the Ria de Arousa) (Figures 1 and 7), whose upper levels of sands were deposited 2.5 ky ago (López-Romero et al., 2020). These dunes of the Areoso Islet, now being eroded by wind and waves, fossilize a 6 ky-old megalithic monument (López-Romero et al., 2020; Mañana-Borrazás et al., 2020). Surprisingly, these partially flooded dunes also fossilize an organic soil of continental origin that includes woody macrofossils dated back to 3.7 ky cal BP (Blanco-Chao et al., 2017; Cajade-Pascual et al., 2019) (Table 2), an age in good agreement with the submerged-forest soils mentioned above (Figure 10). All this indicates a fully emerged islet connected to the mainland, with the presence of human activity and well-developed forests buried by the dune fields (López-Romero et al., 2020). Bathymetric data (EMODnet, 2018) and the location of the present islet suggest that, for these circumstances to occur, the seashore was far below its current level 3 ky ago (Figure 11). This is also suggested by foraminiferal analysis in the nearest Ria de Vigo (southern Galicia) (Diz et al., 2002).

Once the sea reached its current level, sand supply was completely suspended and the aeolian accretion ended (Figure 11). At this point the wind became exclusively erosive. This is evidenced by blow-out erosive formations (Figures 2b and 9) (see Section 7.2.1) that originate when strong coastal winds strip the vegetation cover from the dune front during storm periods. Aeolian sand infilling of those freshwater coastal lagoons that had not been completely flooded by the sea (Bao et al., 2007; Costas et al., 2009; González-Villanueva et al., 2015; Sáez et al., 2018; Santos & Vidal-Romaní, 1993) also indicates the erosion of the dunes by wind (Table 2). At present, dune fields on the coast of Galicia no longer receive supplies as they did thousands of years ago, and under a temperate-humid climate such as that of NW Spain (Fick & Hijmans, 2017) they are colonized by terrestrial vegetation (Jackson et al., 2019), temporarily protecting them from erosion. The reactivation of aeolian accretion leading to new dune fields, or the advance of pre-existing dunes over the current vegetation cover, are not observed today (Flor-Blanco et al., 2021). Nor is it observed that coastal vegetation leads to the formation of dunes (e.g. nebka type) (Durán & Moore, 2013; Hesp et al., 2021), as proposed for other coastal areas of different morphological, sedimentary, tidal and/or dissipative characteristics. On the contrary, it is terrestrial vegetation—including forest vegetation such as *Pinus* sp. (Gómez-Serrano et al., 2009; Muñoz-Reinoso, 2021)—that today colonizes the dune fields, previously transformed into relict formations due to the lack of sand supply, as mentioned. This novel historical and evolutionary perspective on coastal dunes in NW Spain provides insight into the vulnerability of these relict sand sediments to major storms associated with more recent extreme events linked to global warming.

## 8 | CONCLUSIONS

Morphological, microscopic and grain size analyses show an aeolian origin for the sandy deposits studied here. OSL dating establishes a formation age for these outcrops between 35 and 14 ky, at the end of the last glacial episode (MIS2). The location of these aeolianites and the lack of sedimentary structures suggest that they are climbing dunes.

During the period of accumulation of these dunes at the end of the Upper Pleistocene, the sea level was supposed to be −120 m bmsl on this coast. This means a shoreline displaced by several kilometres and the subaerial exposure of a wide strip of the continental shelf covered by sands which were later transported by the coastal winds towards the continent, then reaching the areas where the tidal processes are currently developing. According to the local record, the magnitude of the aeolian accretion at the end of the last glacial period allowed the advance of the dunes that in some cases reached a height of 300 m, causing the collapse of coastal ecosystems.

The mobilization of dunes just stopped when the sea reached its present level and the ocean flooded the source areas of aeolian sands less than 3 ky ago. From this moment the wind became a purely erosive agent, eroding sand from a large part of the dunes that were previously formed. At present, on the Atlantic coast of Galicia, with a high-energy dissipation, waves also destroy the Late Pleistocene and Holocene coastal aeolian formations (dunes), favouring the exposure of the old shingle beaches, old forests and megalithic monuments.

In a global warming context, the rise in sea level inherent to the current interglacial episode (Holocene) had initially favoured the formation of the dune fields, but has led to their subsequent flooding, reworking and marine erosion. According to the hypotheses proposed here, all the dunes preserved today in the study area are relict aeolian formations, generally impeded by vegetation and very vulnerable to the most extreme climatic events. This evolution model could be extrapolated to the southern half of the European Atlantic coast, being a critical issue for the future management of these coastal ecosystems.

### ACKNOWLEDGEMENTS

This research has been funded and supported by Consellería de Cultura, Educación e Ordenación Universitaria, Xunta de Galicia (programmes ED431B 2018/47 and ED431B 2021/17)

through the Grupo Interdisciplinar de Patrimonio Cultural e Xeolóxico (CULXEO). Thanks to Universidade da Coruña/Consorcio Interuniversitario del Sistema Universitario de Galicia (CISUG) for Open Acces funding.

## AUTHOR CONTRIBUTIONS

Conceptualization (CAC, JRVR and AGdG), funding adquisition (JRVR and AGdG), methodology (CAC and JSS), investigation and resources (CAC and JRVR), supervision (JRVR and JSS) and writing (CAC and JRVR).

## DATA AVAILABILITY STATEMENT

The data that support the findings of this study are openly available at the Repository of Universidade da Coruña (RUC) (http://hdl.handle.net/2183/19810).

## ORCID

*Carlos Arce Chamorro* https://orcid.org/0000-0001-5374-5485

## REFERENCES

Alonso, A. & Pagés, J.L. (2000) El registro sedimentario del final del Cuaternario en el NW de la Península Ibérica. Márgenes Cantábrico y Atlántico. *Revista de la Sociedad Geológica de España*, 13, 17–29.

Alonso, A. & Pagés, J.L. (2010) Evolución del nivel del mar durante el Holoceno en el noroeste de la Península Ibérica. *Revista de la Sociedad Geológica de España*, 23, 157–167. Available from: https://sge.usal.es/archivos/REV/23(3-4)/art05.pdf

Arce-Chamorro, C. (2017) *Datación por luminiscencia de depósitos fluviales y eólicos en el margen occidental de Galicia*. PhD thesis, Universidade da Coruña, Spain.

Arce-Chamorro, C., Vidal-Romaní, J.R. & Sanjurjo-Sánchez, J. (2021) Islas Cíes: una trampa eólica en la Ría de Vigo (NO de la Península Ibérica) al final del último glacial. Estudio del afloramiento de eolianitas de la Isla de Monteagudo (Cíes, Pontevedra, Galicia). *Geogaceta*, 70, 3–6.

Banerjee, D., Bøtter-Jensen, L. & Murray, A.S. (2000) Retrospective dosimetry: Estimation of the dose to quartz using the single-aliquot regenerative-dose protocol. *Applied Radiation and Isotopes*, 52(4), 831–844. Available from: https://doi.org/10.1016/S0969-8043(99)00247-X

Bao, R., Alonso, A., Delgado, D. & Pagés, J.L. (2007) Identification of the main driving mechanisms in the evolution of a small coastal wetland (Traba, Galicia, NW Spain) since its origin 5700 cal yr BP. *Palaeogeography, Palaeoclimatology, Palaeoecology*, 247(3–4), 296–312. Available from: https://doi.org/10.1016/j.palaeo.2006.10.019

Bertran, P., Andrieux, E., Bateman, M.D., Fuchs, M., Klinge, M. & Marembert, F. (2020) Mapping and chronology of coversands and dunes from the Aquitaine basin, Southwest France. *Aeolian Research*, 47, 100628. Available from: https://doi.org/10.1016/j.aeolia.2020.100628

Bickel, L., Lüthgens, C., Lomax, H. & Fiebig, M. (2015) Luminescence dating of glaciofluvial deposits linked to the penultimate glaciation in the eastern Alps. *Quaternary International*, 357, 110–124. Available from: https://doi.org/10.1016/j.quaint.2014.10.013

Bicket, A. & Tizzard, L. (2015) A review of the submerged prehistory and palaeolandscapes of the British isles. *Proceedings of the Geologists Association*, 126(6), 643–663. Available from: https://doi.org/10.1016/j.pgeola.2015.08.009

Blanco-Chao, R., Costa-Casais, M., Taboada-Rodríguez, T. & Tallón-Armada, R. (2017) Sedimentología y cambios del nivel del mar en el islote Guidoiro Areoso, Ría de Arousa, NO de la Península Ibérica. *Geotemas*, 17, 103–106.

Bosq, M., Bertran, P., Beauval, C., Kreutzer, S., Duval, M., Bartz, M., Mercier, N., Sitzia, L. & Stéphan, P. (2019) Stratigraphy and chronology of Pleistocene coastal deposits in northern Aquitaine, France: A reinvestigation. *Quaternaire*, 30(1), 275–303. Available from: https://doi.org/10.4000/quaternaire.11112

Brennan, B.J. (2003) Beta doses to spherical grains. *Radiation Measurements*, 37(4–5), 299–303. Available from: https://doi.org/10.1016/S1350-4487(03)00011-8

Bronk-Ramsey, C. (2009) Bayesian analysis of radiocarbon dates. *Radiocarbon*, 51, 337–360. Available from: https://doi.org/10.1017/S0033822200033865

Brown, S., Hanson, S. & Nicholls, R.J. (2014) Implications of sea-level rise and extreme events around Europe: A review of coastal energy infrastructure. *Climatic Change*, 122(1–2), 81–95. Available from: https://doi.org/10.1007/s10584-013-0996-9

Burow, C., Kreutzer, S., Dietze, M., Fuchs, M.C., Fischer, M., Schmidt, C. & Brückner, H. (2016) RLumShiny – a graphical user interface for the R package 'Luminescence'. *Ancient TL*, 34, 22–32.

Cajade-Pascual, D., Costa-Casais, M. & Blanco-Chao, R. (2019) Ascenso del nivel del mar y cambios ambientales costeros durante el Holoceno Final. Islote Areoso, Ría de Arousa. In: Durán, R., Guillén, L. & Simarro, G. (Eds.) *X Jornadas de Geomorfología Litoral. Libro de ponencias. Castelldefels, 4–6 septiembre*. Spain: CSIC, pp. 261–264. Available from: https://doi.org/10.20350/digitalCSIC/8956

Caraballo-Muziotti, L.F. (1969) *Estudio fisiográfico-sedimentológico de las rías y frente costero comprendidos entre la Estaca de Vares y el Cabo Prior (Provincia de La Coruña)*. PhD thesis, Universidad Complutense, Spain.

Cartelle, V. (2018) *Stratigraphy, depositional environments, shallow gas and seismic-sequential analysis of the sedimentary record of the rias of Arousa and Ferrol*. PhD thesis, Universidade de Vigo, Spain.

Cawthra, H.C., Jacobs, Z. & Wadley, L. (2022) Winds of change: Climate variability in a mild glacial on the east coast of South Africa, inferred from submerged aeolianites and the archaeological record of Sibudu. *Quaternary International*, 638–639, 23–36. Available from: https://doi.org/10.1016/j.quaint.2022.03.014

Costa-Casais, M. & Caetano-Alves, M.I. (2013) Geological heritage at risk in NW Spain. Quaternary deposits and landforms of "southern coast" (Baiona-a Garda). *Geoheritage*, 5(4), 227–248. Available from: https://doi.org/10.1007/s12371-013-0083-7

Costas, S., Jerez, S., Trigo, R.M., Bogle, R. & Rebêlo, L. (2012) Sand invasion along the Portuguese coast forced by westerly shifts during cold climate events. *Quaternary Science Reviews*, 42, 15–28. Available from: https://doi.org/10.1016/j.quascirev.2012.03.008

Costas, S., Muñoz-Sobrino, C., Alejo, I. & Pérez-Arlucea, M. (2009) Holocene evolution of a rock-bounded barrier–lagoon system, Cies Islands, Northwest Iberia. *Earth Surface Processes and Landforms*, 34(11), 1575–1586. Available from: https://doi.org/10.1002/esp.1849

De Vicente, G. & Vegas, R. (2009) Large-scale distributed deformation controlled topography along the western Africa–Eurasia limit: Tectonic constrains. *Tectonophysics*, 474(1–2), 124–143. Available from: https://doi.org/10.1016/j.tecto.2008.11.026

De Winter, R.C. & Ruessink, B.G. (2017) Sensitivity analysis of climate change impacts on dune erosion: Case study for the Dutch Holland coast. *Climatic Change*, 141(4), 685–701. Available from: https://doi.org/10.1007/s10584-017-1922-3

Devoy, R.J.N., Delaney, C., Carter, R.W.G. & Jennings, S.C. (1996) Coastal stratigraphies as indicators of environmental changes upon European coasts in the Late Holocene. *Journal of Coastal Research*, 12, 564–588.

Dias, J.M.A., González, R., García, C. & Díaz-del Río, V. (2002) Sediment distribution patterns on the Galicia-Minho continental shelf. *Progress in Oceanography*, 52(2–4), 215–231. Available from: https://doi.org/10.1016/S0079-6611(02)00007-1

Diz, P., Francés, G., Pelejero, C., Grimalt, J.O. & Vilas, F. (2002) The last 3000 years in the Ría de Vigo (NW Iberian margin): Climatic and hydrographic signals. *The Holocene*, 12(4), 459–468. Available from: https://doi.org/10.1191/0959683602hl550rp

Duque, L.C., Elízaga, E. & Vidal Romaní, J.R. (1983) *Puntos de Interés Geológico de Galicia*. Madrid: Instituto Geológico y Minero de España.

Durán, O. & Moore, L.J. (2013) Vegetation controls on the maximum size of coastal dunes. *PNAS*, 43, 17217–17222. Available from: https://doi.org/10.1073/pnas.1307580110

Durán, R. (2005) *Estratigrafía sísmica desde el último máximo glacial en la Ría de Pontevedra (NO de España)*. PhD thesis, Universidade de Vigo, Spain.

EMODnet. (2018) EMODnet Digital Bathymetry (DTM). https://doi.org/10.12770/18ff0d48-b203-4a65-94a9-5fd8b0ec35f6

Engel, M., May, S.M., Scheffers, A., Squire, P., Pint, A., Kelletat, D. & Brückner, H. (2015) Prograded foredunes of Western Australia's macro-tidal coast – implications for Holocene sea-level change and high-energy wave impacts. *Earth Surface Processes and Landforms*, 40(6), 726–740. Available from: https://doi.org/10.1002/esp.3663

Fick, S.E. & Hijmans, R.J. (2017) WorldClim 2: New 1-km spatial resolution climate surfaces for global land areas. *International Journal of Climatology*, 37(12), 4302–4315. Available from: https://doi.org/10.1002/joc.5086

Flor-Blanco, G., Alcántara-Carrió, J., Jackson, D.W.T., Flor, G. & Flores-Soriano, C. (2021) Coastal erosion in NW Spain: Recent patterns under extreme storm wave events. *Geomorphology*, 387, 107767. Available from: https://doi.org/10.1016/j.geomorph.2021.107767

Galbraith, R.F. & Roberts, R.G. (2012) Statistical aspects of equivalent dose and error calculation and display in OSL dating: An overview and some recommendations. *Quaternary Geochronology*, 11, 1–27. Available from: https://doi.org/10.1016/j.quageo.2012.04.020

Galbraith, R.F., Roberts, R.G., Laslett, G.M., Yoshida, H. & Olley, J.M. (1999) Optical dating of single and multiple grains of quartz from Jinmium rock shelter, northern Australia: Part I. Experimental design and statistical models. *Archaeometry*, 41(2), 339–364. Available from: https://doi.org/10.1111/j.1475-4754.1999.tb00987.x

García-Amorena, I., Gómez-Manzaneque, F., Rubiales, J.M., Granja, H.M., de Carvalho, G.S. & Morla, C. (2007) The Late Quaternary coastal forests of western Iberia: A study of their macroremains. *Palaeogeography, Plaeoclimatology, Palaeoecology*, 254(3–4), 448–461. Available from: https://doi.org/10.1016/j.palaeo.2007.07.003

García-Gil, S., Cartelle, V., Muñoz-Sobrino, C., Martínez-Carreño, N. & García-Moreiras, I. (2020) Sedimentary conditioning of a rocky strait during the Holocene transgression: Ría de Ferrol (NW Spain). https://doi.org/10.5194/egusphere-egu2020-10493

García-Gil, S., Vilas-Martín, F., Muñoz, A., Acosta, J. & Uchupi, E. (1999) Quaternary sedimentation in the Ría de Pontevedra (Galicia), Northwest Spain. *Journal of Coastal Research*, 15, 1083–1090. Available from: https://www.jstor.org/stable/4299026

García-Moreiras, I., Delgado, C., Martínez-Carreño, N., García-Gil, S. & Muñoz Sobrino, C. (2019) Climate and vegetation changes in coastal ecosystems during the middle Pleniglacial and the early Holocene: Two multi-proxy, high-resolution records from ria de Vigo (NW Iberia). *Global and Planetary Change*, 176, 100–122. Available from: https://doi.org/10.1016/j.gloplacha.2019.02.015

Gómez-Orellana, L., Ramil-Rego, P., Badal, E., Carrión, Y. & Muñoz-Sobrino, C. (2014) Mid-Holocene vegetation dynamics in the Tejo River estuary based on palaeobotanical records from Ponta da Passadeira (Barreiro–Setúbal, Portugal). *Boreas*, 43, 792–806. Available from: https://doi.org/10.1111/bor.12068

Gómez-Orellana, L., Ramil-Rego, P., Ferreiro da Costa, J. & Muñoz-Sobrino, C. (2021) Holocene environmental change on the Atlantic coast of NW Iberia as inferred from the Ponzos wetland sequence. *Boreas*, 50(4), 1131–1145. Available from: https://doi.org/10.1111/bor.12535

Gómez-Orellana, L., Ramil-Rego, P. & Muñoz Sobrino, C. (2007) The Würm in NW Iberia, a pollen record from Area Longa (Galicia). *Quaternary Research*, 67(3), 438–452. Available from: https://doi.org/10.1016/j.yqres.2007.01.003

Gómez-Serrano, M.A., Sanjaume, E. & Gracia Prieto, F.J. (2009) Dunas con bosques de *Pinus pinea* y/o *Pinus pinaster* (2270). In *VV.AA. Bases ecológicas preliminares para la conservación de los tipos de hábitat de interés comunitario en España*. Ministerio de Medio Ambiente, y Medio Rural y Marino: Madrid.

González-Villanueva, R., Pérez-Arlucea, M., Costas, S., Bao, R., Otero, X. L. & Goble, R. (2015) 8000 years of environmental evolution of barrier–lagoon systems emplaced in coastal embayments (NW Iberia). *The Holocene*, 25(11), 1786–1801. Available from: https://doi.org/10.1177/0959683615591351

Google Earth. (2020) Terrametrics. https://www.google.com/intl/es/earth/

Gracia, J., Del Río, L., Alonso, C., Benavente, J. & Anfuso, G. (2006) Historical evolution and present state of the coastal dune systems in the Atlantic coast of Cádiz (SW Spain): Palaeoclimantic and environmental implications. *Journal of Coastal Research*, 48, 55–63.

Granja, H.M. & Soares de Carvalho, G. (1995) Sea-level changes during the Pleistocene–Holocene in the NW coastal zone of Portugal. *Terra Nova*, 7(1), 60–67. Available from: https://doi.org/10.1111/j.1365-3121.1995.tb00668.x

Greeley, R. & Iversen, J.D. (1985) *Wind as a Geological Process on Earth, Mars, Venus and Titan*. Cambridge: Cambridge University Press. Available from: https://doi.org/10.1017/CBO9780511573071

Guérin, G. & Mercier, N. (2012) Preliminary insight into dose deposition processes in sedimentary media on a scale of single grains: Monte Carlo modelling of the effect of water on the gamma dose rate. *Radiation Measurements*, 47(7), 541–547. Available from: https://doi.org/10.1016/j.radmeas.2012.05.004

Guérin, G., Mercier, N. & Adamiec, G. (2011) Dose rate conversion factors. *Ancient TL*, 29, 5–8.

Gutiérrez-Becker, L. (2008) *Caracterización de los sistemas dunares costeros del NW ibérico y su evolución durante el Cuaternario*. PhD thesis, Universidad de Coruña, Spain.

Hardt, J., Lüthgens, C., Hebenstreit, R. & Böse, M. (2016) Geochronological (OSL) and geomorphological investigations at the presumed Frankfurt ice marginal position in Northeast Germany. *Quaternary Science Reviews*, 154, 85–99. Available from: https://doi.org/10.1016/j.quascirev.2016.10.015

Hay, A.S., Powell, D.M., Carr, A.S. & Livinsgstone, I. (2021) Characterisation of aeolian sediment accumulation and preservation across complex topography. *Geomorphology*, 383, 107704. Available from: https://doi.org/10.1016/j.geomorph.2021.107704

Hesp, P.A., Hernández-Calvento, L., Gallego-Fernández, J.B., Miot da Silva, G., Hernández-Cordero, A.I., Ruz, M.H. & Romero, L.G. (2021) Nebkha or not? Climate control on foredune mode. *Journal of Arid Environments*, 187, 104444. Available from: https://doi.org/10.1016/j.jaridenv.2021.104444

IGME. (2004) *Mapa Geológico de España, 1:25,000*. Hoja 1104 IV. Instituto Geológico y Minero de España: Madrid.

Jackson, D.W.T., Costas, S., González-Villanueva, R. & Cooper, A. (2019) A global 'greening' of coastal dunes: An integrated consequence of climate change? *Global and Planetary Change*, 182, 103026. Available from: https://doi.org/10.1016/j.gloplacha.2019.103026

Jacobs, Z. (2008) Luminescence chronologies for coastal and marine sediments. *Boreas*, 37(4), 508–535. Available from: https://doi.org/10.1111/j.1502-3885.2008.00054.x

Leira, M., Freitas, M.C., Ferreira, T., Cruces, A., Connor, S., Andrade, C., Lopes, V. & Bao, R. (2019) Holocene sea level and climate interactions on wet dune slack evolution in SW Portugal: A model for future scenarios? *The Holocene*, 29(1), 26–44. Available from: https://doi.org/10.1177/0959683618804633

Ley, C., Gallego, J.B. & Vidal, C. (2007) *Manual de restauración de dunas costeras*. Dirección General de Costas, Ministerio de Medio Ambiente: Spain. https://www.miteco.gob.es/es/costas/publicaciones/cap01_introduccion_tcm30-161387.pdf

Lisiecki, L.E. & Raymo, M.E. (2005) A Pliocene–Pleistocene stack of 57 globally distributed benthic $\delta^{18}O$ records. *Paleoceanography*, 20, PA1003. Available from: https://doi.org/10.1029/2004PA001071

Lommertzen, K. (2011) *Landscape genesis. Marine and river terraces around the Miño Estuary*. PhD thesis, Wageningen University and Research Centre and Universidade da Coruña, Spain.

López-Cancelo, L. (2004) *Cambios paleoambientales en el NW peninsular, durante el Holoceno, determinados a partir del estudio de foraminíferos bentónicos*. PhD thesis, Universidad de A Coruña, Spain.

López-Romero, E., Bóveda-Fernández, M.J., Güimil-Fariña, A., Mañana-Borrazás, P., Sanjurjo-Sánchez, J., Vázquez-Collazo, S. & Vilaseco-Vázquez, X.I. (2020) Prehistoric human occupation in the Western Rias of Galicia (Norwest Iberia): A review of methods and prospects. In *Proceedings of the 1st International Webinar: Investigate the Shore, Sound the Past. New Methods and Practices of Maritime Prehistory*. IRN PrehCOAST – French Prehistoric Society: Brest.

Loureiro, C., Ferreira, O. & Cooper, J.A.G. (2012) Extreme erosion on high-energy embayed beaches: Influence of megarips and storm grouping. *Geomorphology*, 139–140, 155–171. Available from: https://doi.org/10.1016/j.geomorph.2011.10.013

Mañana-Borrazás, P., Blanco-Chao, R., Bóveda-Fernández, M. & Cajade-Pascual, D. (2020) Lo que nos cuenta la marea. Prehistoria en el islote de Guidoiro Areoso (A Illa de Arousa, Galicia) a la luz de las últimas intervenciones. In *Actualidad de la investigación arqueológica en España*; 159–176. http://www.man.es/man/estudio/publicaciones/conferencias-congresos/2020-aae.html

Marrero-Rodríguez, N. & Dóniz-Páez, J. (2022) Coastal dunes geomorphosites to develop the geotourism in a volcanic subtropical oceanic island, Tenerife, Spain. *Land*, 11(3), 426. Available from: https://doi.org/10.3390/land11030426

Martínez-Carreño, M. & García-Gil, S. (2013) The Holocene gas system of the Ría de Vigo (NW Spain): Factors controlling the location of gas accumulations, seeps and pockmarks. *Marine Geology*, 344, 82–100. Available from: https://doi.org/10.1016/j.margeo.2013.07.012

Martínez-Carreño, M. & García-Gil, S. (2017) Reinterpretation of the quaternary sedimentary infill of the Ría de Vigo, NW Iberian Peninsula, as a compound incised valley. *Quaternary Science Reviews*, 173, 124–144. Available from: https://doi.org/10.1016/j.quascirev.2017.08.015

Martínez-Carreño, M., García-Gil, S. & Cartelle, V. (2017) An unusual Holocene fan-shaped subaqueous prograding body at the back of the Cíes Islands ridge (Ría de Vigo, NW Spain): Geomorphology, facies and stratigraphic architecture. *Marine Geology*, 385, 13–26. Available from: https://doi.org/10.1016/j.margeo.2016.11.015

Méndez, G. & Vilas, R. (2005) Geological antecedents of the rias Baixas (Galicia, Northwest Iberian Peninsula). *Journal of Marine Systems*, 54(1–4), 195–207. Available from: https://doi.org/10.1016/j.jmarsys.2004.07.012

Mohamed, K.J., Rey, D., Rubio, B., Vilas, F. & Frederichs, T. (2010) Interplay between detrital and diagenetic processes since the last glacial maximum on the northwest Iberian continental shelf. *Quaternary Research*, 73(3), 507–520. Available from: https://doi.org/10.1016/j.yqres.2010.02.003

Mosquera-Santé, M.J. (2000) *Evolución post-glaciar del nivel del mar en el NO de la Península Ibérica: El caso del golfo Ártabro*. PhD thesis, Universidad de A Coruña, Spain.

Moura, D., Veiga-Pires, C., Albardeiro, L., Boski, T., Rodrigues, A.L. & Tareco, H. (2007) Holocene sea level fluctuations and coastal evolution in the Central Algarve (southern Portugal). *Marine Geology*, 237(3–4), 127–142. Available from: https://doi.org/10.1016/j.margeo.2006.10.026

Muñoz-Reinoso, J.C. (2021) Effects of pine plantations on coastal gradients and vegetation zonation in SW Spain. *Estuarine, Coastal and Shelf Science*, 251, 107082. Available from: https://doi.org/10.1016/j.ecss.2021.107182

Muñoz-Salinas, E., Castillo, M., Caballero, L. & Lacan, P. (2017) Understanding landscape dynamics of the Sierra Juarez, Southern Mexico: An exploratory approach using inherited luminescence signals. *Journal of South American Earth Sciences*, 76, 208–217. Available from: https://doi.org/10.1016/j.jsames.2017.03.001

Muñoz-Sobrino, C., García-Moreiras, I., Martínez-Carreño, N., Cartelle, V., Lado Insua, T., Ferreiro da Costa, J., Ramil-Rego, P., Fernández-Rodrígues, C., Alejo, I. & Garcia-Gil, N. (2016) Reconstruction of the environmental history of a coastal insular system using shallow marine records: The last three millennia of the Cíes Islands (Ría de Vigo, NW Iberia). *Boreas*, 45(4), 729–753. Available from: https://doi.org/10.1111/bor.12178

Muñoz-Vallés, S. & Cambrollé, J. (2014) Successes and failures in the management of coastal dunes of SW Spain: Status analysis nine years after management decisions. *Ecological Engineering*, 71, 415–425. Available from: https://doi.org/10.1016/j.ecoleng.2014.07.042

Murray, A.S. & Wintle, A.G. (2000) Luminescence dating of quartz using an improved single-aliquot regenerative-dose protocol. *Radiation Measurements*, 32(1), 57–73. Available from: https://doi.org/10.1016/S1350-4487(99)00253-X

NASA. (2000) *SRTM90m Digital Elevation Data from the CGIAR-CSI Consortium for Spatial Information*. College Park, MD: University of Maryland.

Nathan, R., Thomas, P.J., Murray, A.S. & Rhodes, E.J. (2003) Environmental dose rate heterogeneity of beta radiation and its implications for luminescence dating: Monte Carlo modelling and experimental validation. *Radiation Measurements*, 37(4–5), 305–313. Available from: https://doi.org/10.1016/S1350-4487(03)00008-8

Nieto, M.I. & Vidal-Romaní, J.R. (1989) Niveles marinos y depósitos continentales antiguos en el borde costero entre Cabo Prior y Cabo Prioriño (A Coruña, Galicia, España). *Cadernos Lab. Xeolóxico de Laxe*, 14, 67–78.

Nombela, M.A., Alejo, I., Bernárdez, F., Clemente, F., Costas, S., Diz, P., Fernández-Bastero, S., Francés, G., Gago-Duport, L., García, T., González-Alonso, D., González-Álvarez, R., González-Villanueva, R., Liquete, C., Pena, L.D. & Pérez-Arlucea, M. (2005) Evolución sedimentaria desde el último máximo glacial en la costa y plataforma continental de las Rías Baixas (Galicia, NW de la Península Ibérica) (Talk). In: Freitas, M.C. & Drago, T. (Eds.) *Iberian Coastal Holocene Paleoenvironmental Evolution: Coastal Hope Conference Proceedings, 24–29 July, Lisbon, Portugal*, pp. 99–100. http://hdl.handle.net/10400.9/2804

Nombela, M.A. & Vilas, F. (1987) Medios y submedios en el sector intermareal de la ensenada de San Simón. Ría de Vigo (Pontevedra): secuencias sedimentarias características. *Acta Geológica Hispánica*, 21–22, 223–231.

Nonn, H. (1966) *Les régiones cotières de la Galice (Espagne). Etude géomorpholigique*. Publications de la Faculté des lettres de L'Université de Strasbourg, Foundation Baulig, Tomo III.

Oberle, F.K.J., Hanebuth, T.J.J., Baasch, B. & Schwenk, T. (2014) Volumetric budget calculation of sediment and carbon storage and export for a Late Holocene mid-shelf mudbelt system (NW Iberia). *Continental Shelf Research*, 76, 12–24. Available from: https://doi.org/10.1016/j.csr.2013.12.012

Pardiñas-González, R. (2021) *Cambios en el nivel del mar causados por el Cambio Climático durante el Cuaternario Superior en la Costa de la Provincia de A Coruña*. Final degree project, Universidade da Coruña, Spain.

Pazos, O., Vila, A., Alejo, I., Vilas, F. & Nombela, M.A. (1997) Sedimentos costeros relictos frente a las Rías Bajas. *Thalassas*, 13, 135–141.

Petit, J.R., Jouzel, J., Raynaud, D., Barkov, N.I., Barnola, J.M., Basile, I., Bender, M., Chappellaz, J., Davis, M., Delaygue, G., Delmotte, M., Kotlyakov, V.M., Legrand, M., Lipenkov, V.Y., Lorius, C., Pépin, L., Ritz, C., Saltzman, E. & Stievenard, M. (1999) Climate and atmospheric history of the past 420,000 years from the Vostok ice core, Antarctica. *Nature*, 399(6735), 429–436. Available from: https://doi.org/10.1038/20859

Powers, M.C. (1953) A new roundness scale for sedimentary particles. *Journal of Sedimentary Petrology*, 23, 117–119. Available from: https://doi.org/10.1306/D4269567-2B26-11D7-8648000102C1865D

Prescott, J.R. & Hutton, J.T. (1994) Cosmic ray contribution to dose rates for luminescence and ESR dating: Large depths and long-term time variations. *Radiation Measurements*, 23(2–3), 497–500. Available from: https://doi.org/10.1016/1350-4487(94)90086-8

Pye, K. & Tsoar, H. (1990) *Aeolian Sand and Sand Dunes*. London: Unwin Hyman.

Reimer, P.J., Austin, W.E., Bard, E., Bayliss, A., Blackwell, P.G., Ramsey, C. B., Butzin, M., Cheng, H., Edwards, R.L., Friedrich, M., Grootes, P.M., Guilderson, T.P., Hajdas, I., Heaton, T.J., Hogg, A.G., Hughen, K.A., Kromer, B., Manning, S.W., Muscheler, R., Palmer, J.G., Pearson, C., van der Plicht, J., Reimer, R.W., Richards, D.A., Scott, E.M., Southon, J.R., Turney, C.S.M., Wacker, L., Adolphi, F., Büntgen, U., Capano, M., Fahrni, S.M., Fogtmann-Schulz, A., Friedrich, R., Köhler, P., Kudsk, S., Miyake, F., Olsen, J., Reinig, F., Sakamoto, M., Sookdeo, A. & Talamo, S. (2020) The IntCal20 northern hemisphere radiocarbon age calibration curve (0–55 cal kBP). *Radiocarbon*, 62, 725–757. Available from: https://doi.org/10.1017/RDC.2020.41

Reynard, E., Fontana, G., Kozlik, L. & Scapozza, C. (2007) A method for assessing the scientific and additional values of geomorphosites. *Geographica Helvetica*, 62(3), 148–158. Available from: https://doi.org/10.5194/gh-62-148-2007

Rey-Salgado, J. (1993) *Relación morfosedimentaria entre la Plataforma Continental de Galicia y las Rías Bajas y su evolución durante el Cuaternario*. Trabs. Inst. Esp. Oceanogr. 17, Madrid.

Ribeiro, H., Bernal, A., Flores, D., Pissarra, J., Abreu, I., Romani, J.V. & Noronha, F. (2011) A multidisciplinary study of an organic-rich mudstone in the middle Holocene on the northern coast of Portugal. *Comunicações Geológicas*, 98, 93–98.

Ribeiro, H., Pinto de Jesus, A., Sanjurjo-Sánchez, J., Abreu, I., Vidal Romani, J.R. & Noronha, F. (2019) Multidisciplinary study of the quaternary deposits of the Vila Nova de Gaia, NW Portugal, and its climate significance. *Journal of Iberian Geology*, 45(4), 1–11. Available from: https://doi.org/10.1007/s41513-019-00109-9

Rodríguez-Vidal, J., Bardají, T., Zazo, C., Goy, J.L., Borja, F., Dabrio, C.J., Lario, J., Cáceres, L.M., Ruiz, F. & Abad, M. (2014) Coastal dunes and marshes in Doñana National Park. In: Gutiérrez, F. & Gutiérrez, M. (Eds.) *Landscapes and Landforms of Spain*. Dordrecht: Springer, pp. 229–238.

Rodríguez-Vidal, J., Cáceres, L.M., Finlayson, J.C., Gracia, F.J. & Martínez-Aguirre, A. (2004) Neotectonics and shoreline history of the rock of Gibraltar, southern Iberia. *Quaternary Science Reviews*, 23(18–19), 2017–2029. Available from: https://doi.org/10.1016/j.quascirev.2004.02.008

Roettig, C.B., Kolb, T., Wolf, D., Baumgart, P., Richter, C., Schleicher, A., Zöller, L. & Faust, D. (2017) Complexity of quaternary aeolian dynamics (Canary Islands). *Palaeogeography, Palaeoclimatology, Palaeoecology*, 472, 146–162. Available from: https://doi.org/10.1016/j.palaeo.2017.01.039

Rosón, G., Cabanas, J.M. & Fiz, F. (2008) Hidrografía y dinámica de la Ria de Vigo. Un sistema de afloramiento. In *Proceedings Hydrography*. http://hdl.handle.net/10261/115885

Sáez, A., Carballeira, R., Pueyo, J.J., Vázquez-Loureiro, D., Leira, M., Hernández, A., Valero-Garcés, B.L. & Bao, R. (2018) Formation and evolution of back-barrier perched lakes in rocky coasts: An example of a Holocene system in North-West Spain. *Sedimentology*, 65(6), 1891–1917. Available from: https://doi.org/10.1111/sed.12451

Salvany, J.M., Larrasoaña, J.C., Mediavilla, C. & Rebollo, A. (2011) Chronology and tectono-sedimentary evolution of the Upper Pliocene to Quaternary deposits of the lower Guadalquivir foreland basin, SW Spain. *Sedimentary Geology*, 241(1–4), 22–39. Available from: https://doi.org/10.1016/j.sedgeo.2011.09.009

Santos, M.L. & Vidal-Romaní, J.R. (1993) El Lagoon de Seselle: un episodio de la transgresión holocena en la Ría de Ares (A Coruña, Galicia, España). Datos geomorfológicos, sedimentarios y paleoecológicos. *Cadernos Lab. Xeolóxico de Laxe*, 18, 163–174.

Sitzia, L., Bertran, P., Bahain, J.J., Bateman, M.D., Hernandez, M., Garon, H., de Lafontaine, G., Mercier, N., Leroyer, C., Queffelec, A. & Voinchet, P. (2015) The quaternary coversands of Southwest France. *Quaternary Science Reviews*, 124, 84–105. Available from: https://doi.org/10.1016/j.quascirev.2015.06.019

Teixeira, C. (1949) Plages anciennes et terrasses fluviatiles du littoral du Nord-Ouest de la Peninsule Iberique. *Boletim do Museu do Laboratorio Mineralogico e Geologico da Universidade de Lisboa*, 17, 33–48.

Thomas, J.P., Murray, A.S., Granja, H.M. & Jain, M. (2006) Optical dating of Late Quaternary coastal deposits in northwestern Portugal. *Journal of Coastal Research*, 24, 134–144. Available from: https://doi.org/10.2112/06-0702.1

Torcal-Sainz, L. & Tello-Ripa, B. (1992) *Análisis de sedimentos con microscopio electrónico de barrido: exoscopía de cuarzo y sus aplicaciones a la geomorfología*. Cuadernos Técnicos de la Sociedad Española de Geomorfología n. 4.

Trauerstein, M., Lowick, S.E., Preusser, F. & Schlunegger, F. (2014) Small aliquot and single grain IRSL and post-IR IRSL dating of fluvial and alluvial sediments from the Pativilca valley, Peru. *Quaternary Geochronology*, 22, 163–174. Available from: https://doi.org/10.1016/j.quageo.2013.12.004

Trindade, M.J., Prudêncio, M.I., Sanjurjo-Sánchez, J., Vidal-Romani, J.R., Ferraz, T., Mosquera, D.F. & Dias, M.I. (2013) Post-depositional processes of elemental enrichment inside dark nodular masses of an ancient aeolian dune from A Coruña, Northwest Spain. *Geologica Acta*, 11, 231–244. Available from: https://doi.org/10.1344/105.000001838

Tyson, S.J. (1999) *Sand ramps or climbing dunes? Identification and palaeoenvironmental significance of aeolian deposits in the Southern Kalahari and Breede River valley, South Africa*. Master's thesis, University of Cape Town, South Africa.

Vandenberghe, J. (2013) Grain size of fine-grained windblown sediment: A powerful proxy for process identification. *Earth-Science Reviews*, 121, 18–30. Available from: https://doi.org/10.1016/j.earscirev.2013.03.001

Vidal-Romaní, J.R., Fernández-Mosquera, D. & Marti, K. (2015) The glaciation of Serra de Queixa-Invernadoiro and Serra do Geres-Xurés, NW Iberia. A critical review and a cosmogenic nuclide (10-Be and 21-Ne) chronology. *Cadernos Lab. Xeolóxico de Laxe*, 38, 25–44.

Vidal-Romaní, J.R. & Grandal-d'Anglade, A. (2018) Nota sobre la última transgresión marina en la costa de Galicia. *Cadernos Lab. Xeolóxico de Laxe*, 40, 229–246. Available from: https://doi.org/10.17979/cadlaxe.2018.40.0.4921

Viveen, W., Braucher, R., Bourlès, D., Schoorl, J.M., Veldkamp, A., van Balen, R.T., Wallinga, J., Fernandez-Mosquera, D., Vidal-Romani, J.R. & Sanjurjo-Sanchez, J. (2012) A 0.65 ma chronology and incision rate assessment of the NW Iberian Miño River terraces based on $^{10}$Be and luminescence dating. *Global and Planetary Change*, 94–95, 82–100. Available from: https://doi.org/10.1016/j.gloplacha.2012.07.001

Vousdoukas, M., Almeida, L.P. & Ferreira, O. (2012) Beach erosion and recovery during consecutive storms at a steep-sloping, meso-tidal beach. *Earth Surface Processes and Landforms*, 37(6), 583–593. Available from: https://doi.org/10.1002/esp.2264

Waelbroeck, C., Labeyrie, L., Michel, E., Duplessy, J.C., McManus, J.F., Lambeck, K., Balbon, E. & Labracherie, M. (2002) Sea-level and deep water temperature changes derived from benthic foraminifera isotopic records. *Quaternary Science Reviews*, 21(1–3), 295–305. Available from: https://doi.org/10.1016/S0277-3791(01)00101-9

Wentworth, C.K. (1922) A scale of grade class terms for clastic sediments. *Journal of Geology*, 30(5), 377–392. Available from: https://doi.org/10.1086/622910

Westley, K. & Woodman, P. (2020) Ireland: Submerged prehistoric sites and landscapes. In: Bailey, G., Galanidou, N., Peeters, H., Jöns, H. & Mennenga, M. (Eds.) *The Archaeology of Europe's Drowned Landscapes*. Cham: Springer, pp. 221–248.

Williams, D.M. & Doyle, E. (2014) Dates from drowned mid-Holocene landscapes on the central western Irish seaboard. *Irish Journal of Earth Sciences*, 32, 23–27. Available from: https://doi.org/10.3318/ijes.2014.32.23

Zazo, C., Mercier, N., Silva, P.G., Dabrio, C.J., Goy, J.L., Roquero, E., Soler, V., Borja, F., Lario, J., Polo, D. & de Luque, L. (2005) Landscape evolution and geodynamic controls in the Gulf of Cadiz (Huelva coast, SW Spain) during the Late Quaternary. *Geomorphology*, 68(3–4), 269–290. Available from: https://doi.org/10.1016/j.geomorph.2004.11.022

**How to cite this article:** Arce Chamorro, C., Vidal Romaní, J.R., Grandal d'Anglade, A. & Sanjurjo Sánchez, J. (2023) Aeolization on the Atlantic coast of Galicia (NW Spain) from the end of the last glacial period to the present day: Chronology, origin and evolution of coastal dunes linked to sea-level oscillations. *Earth Surface Processes and Landforms*, 48(1), 198–214. Available from: https://doi.org/10.1002/esp.5481